AMERICAN SOCIETY FOR MICROBIOLOGY | Journal of Virology®

VIRUS-CELL INTERACTIONS

G-Protein-Coupled Receptor and Ion Channel Genes Used by Influenza Virus for Replication

Nichole Orr-Burks,[a] Jackelyn Murray,[a] Kyle V. Todd,[a] Abhijeet Bakre,[a] Ralph A. Tripp[a]

[a]Department of Infectious Diseases, College of Veterinary Medicine, University of Georgia, Athens, Georgia, USA

ABSTRACT Influenza virus causes epidemics and sporadic pandemics resulting in morbidity, mortality, and economic losses. Influenza viruses require host genes to replicate. RNA interference (RNAi) screens can identify host genes coopted by influenza virus for replication. Targeting these proinfluenza genes can provide therapeutic strategies to reduce virus replication. Nineteen proinfluenza G-protein-coupled receptor (GPCR) and 13 proinfluenza ion channel genes were identified in human lung (A549) cells by use of small interfering RNAs (siRNAs). These proinfluenza genes were authenticated by testing influenza virus A/WSN/33-, A/CA/04/09-, and B/Yamagata/16/1988-infected A549 cells, resulting in the validation of 16 proinfluenza GPCR and 5 proinfluenza ion channel genes. These findings showed that several GPCR and ion channel genes are needed for the production of infectious influenza virus. These data provide potential targets for the development of host-directed therapeutic strategies to impede the influenza virus productive cycle so as to limit infection.

IMPORTANCE Influenza epidemics result in morbidity and mortality each year. Vaccines are the most effective preventive measure but require annual reformulation, since a mismatch of vaccine strains can result in vaccine failure. Antiviral measures are desirable particularly when vaccines fail. In this study, we used RNAi screening to identify several GPCR and ion channel genes needed for influenza virus replication. Understanding the host genes usurped by influenza virus during viral replication can help identify host genes that can be targeted for drug repurposing or for the development of antiviral drugs. The targeting of host genes is refractory to drug resistance generated by viral mutations, as well as providing a platform for the development of broad-spectrum antiviral drugs.

KEYWORDS influenza, siRNA, virology, virus-host interactions

Influenza A viruses (IAVs) and influenza B viruses (IBVs) are members of the *Orthomyxoviridae* family. IAVs and IBVs contain 8 negative-sense, single-stranded viral RNA gene segments, which encode 10 primary viral proteins—PB2, PB1, PA, HA, NP, NA, M1, M2, NS1, and NS2—as well as strain-dependent accessory proteins mediated by frameshifts and alternative splicing events (1–6). Antigenic drift in the hemagglutinin (HA) gene can lead to changes in viral surface proteins and are responsible for seasonal epidemics, whereas genomic reassortment events may result in pandemics (7, 8). The number of influenza virus-associated illnesses and deaths differs by strain and by the length and severity of the influenza season. Globally, influenza epidemics result in numerous hospitalizations and 290,000 to 650,000 deaths per year (9, 10). The most recent pandemic influenza virus strain, H1N1 2009, resulted in >60 million cases, >274,000 hospitalizations, and >12,400 deaths in the United States (11). IAV vaccines require annual reformulation to prevent vaccine failure (12). The 2014–2015 influenza vaccine, composed of A/Texas/50/2012 (H3N2)-, A/California/7/2009 (H1N1)-, and B/Massachusetts/2/2012-like strains, had low efficacy against the IAV H3N2 strains, largely due to drift events, which most likely occurred postselection (13).

Citation Orr-Burks N, Murray J, Todd KV, Bakre A, Tripp RA. 2021. G-protein-coupled receptor and ion channel genes used by influenza virus for replication. J Virol 95:e02410-20. https://doi.org/10.1128/JVI.02410-20.

Editor Stacey Schultz-Cherry, St. Jude Children's Research Hospital

Address correspondence to Ralph A. Tripp, ratripp@uga.edu.

Received 17 December 2020
Accepted 24 January 2021
Accepted manuscript posted online 3 February 2021
Published 12 April 2021

Viruses exploit host genes and their pathways to support entry, replication, and egress. Some of the most studied pathways exploited by influenza virus include the nuclear factor kappa B (NF-κB), phosphatidylinositol 3-kinase (PI3K), mitogen-activated protein kinase (MAPK), protein kinase C/protein kinase R (PKC/PKR), toll-like receptor (TLR), and retinoic acid-inducible gene 1 (RIG-I) pathways (14–17). Anti-influenza drugs typically target viral proteins, but often these drugs can have reduced efficacy due to drug resistance acquired through antigenic shift and drift (18). For example, amantadine is no longer recommended for the treatment of influenza virus infection due to increased drug resistance, and the reduced efficacy observed for oseltamivir is linked to neuraminidase (NA) mutations (19), creating inconsistencies among therapies (20). In contrast, therapeutics targeting host genes necessary for virus replication could offer an approach refractory to drug resistance while providing broader-spectrum drug efficacy.

RNA interference (RNAi) is a conserved mechanism of posttranscriptional gene-specific regulation (21). RNAi can probe the virus-host interface to identify host genes necessary for virus replication (22–26). Genome-wide RNAi screening has uncovered key virus-host interactions, has helped identify drug targets for influenza viruses (27), and has been used to validate host genes important for virus replication (28–32). Small interfering RNAs (siRNAs) mediate posttranscriptional gene silencing via sequence-specific nucleolytic cleavage or translational inhibition upon interaction with their target mRNAs (29). siRNAs are rationally designed to be specific for one mRNA target (33).

G-protein-coupled receptors (GPCRs) are a family of seven-transmembrane cell surface receptor proteins that facilitate intracellular communication via activation of signal transduction pathways (34). Viruses use GPCRs to facilitate attachment, entry, replication, and egress. For example, HIV tropism is associated with the CXCR4/CCR5 coreceptor and GPCR15 (35–37). In addition, blocking of select GPCRs with drug antagonists obstructs Marburg virus and Ebola virus cell entry and replication (38). The overarching influence of GPCRs on the cell makes drugs that target GPCRs amenable to disease intervention. Similarly, ion channels (ICs) are assemblages of integral protein domains that allow transmembrane passage between the extracellular and intracellular components of the cell (39). ICs enable the influx/efflux of Na^+, K^+, Cl^-, or Ca^{2+} ions, which regulate effector pathways. For example, inhibition of K^+ channels at the early stages of Bunyamwera virus infection hinders virus replication postentry (40). In addition, Cl^- channels are important for herpes simplex virus 1 entry and virus-host fusion (41). Further, the Na^+ channel opener SDZ-201106 can inhibit IAV replication via PKC pathway inhibition (42), and modulation of Cl^- or Na^+ secretion/absorption in the respiratory tract contributes to the regulation of respiratory disease (43).

In this study, we used RNAi as a tool to survey the virus-host interface connected to GPCR and IC genes needed for influenza virus replication. Using siRNA pools to mediate RNAi, we examined GPCR and IC genes for their effects on influenza virus replication in A549 cells based on the following: (i) Z-score, (ii) Ingenuity Pathway Analysis software (2014) (IPA; Qiagen, Inc., Valencia, CA; Qiagen Knowledge Base; Qiagen.com; i.e., searching public databases and published texts), (iii) the availability of small-molecule inhibitors and antagonists, and (iv) targeting by microRNAs (miRs). The gene hits from the RNAi screen of A/WSN/33-infected A549 cells were validated following deconvolution using A/WSN/33. Confirmed hits were reexamined using A/CA/04/09- or B/Yamagata/16/1988-infected A549 cells. The findings from this study provide a better understanding of the virus-host interface and host genes needed for influenza virus replication and provide drug target information for the development of new drugs, or for the repurposing of existing FDA-approved drugs, to combat influenza.

RESULTS

An RNAi screen identifies GPCR genes. GPCR genes permit intracellular communication via signal transduction following activation (34) and are involved in virus replication (38, 44–46). We performed a genome-wide RNAi screen of GPCR genes required

TABLE 1 GPCR genes from a genome-wide RNAi screen

Gene	Function	Z-score[a]
ADGRF1	G-protein-coupled receptor 110	−2.0
ADORA1	Adenosine A1 receptor	−2.1
ADRB2	Adrenoceptor beta 2, surface	−1.8
AGTR1	Angiotensin II receptor, type 1	−1.6
C5AR2	Complement component 5a receptor 2	−1.9
CCKBR	Cholecystokinin B receptor	−2.8
FFAR1	Free fatty acid receptor 1	−2.1
HCAR3	Hydroxycarboxylic acid receptor 3	−1.8
HCRTR2	Hypocretin (orexin) receptor 2	−1.9
HRH2	Histamine receptor H2	−2.3
HTR1B	5-Hydroxytryptamine (serotonin) receptor 1B, G protein coupled	−1.5
LGR4	Leucine-rich repeat containing G-protein-coupled receptor 4	−1.6
LPAR3	Lysophosphatidic acid receptor 3	−1.6
MTNR1B	Melatonin receptor 1B	−1.7
NMUR2	Neuromedin U receptor 2	−1.7
OXGR1	Oxoglutarate (alpha-ketoglutarate) receptor 1	−1.3
OXTR	Oxytocin receptor	−1.4
P2RY12	Purinergic receptor P2Y, G protein coupled, 12	−1.5
PRLHR	Prolactin-releasing hormone receptor	−1.9

[a]A negative Z-score indicates a proinfluenza gene.

for influenza virus replication in A549 cells. Briefly, A549 cells were reverse transfected with siRNA SMARTpools, and 48 h posttransfection, the cells were infected (multiplicity of infection [MOI], 0.001) with A/WSN/33. The levels of virus replication were determined, and a Z-score was applied that showed the number of standard deviations by which the gene knockdown event differed from the mean. A negative Z-score (≤ -1.0) indicated decreased virus replication, while a positive Z-score (≥ 1.0) indicated increased viral replication. Our study focused on gene knockdown events that decreased influenza virus titers, since the goal was to determine strategies for host cell-targeted antiviral therapeutics.

We identified 185 GPCR genes whose knockdown resulted in Z-scores of ≤ -1.0. Further evaluation of these genes with IPA and Gene Ontology (GO) analyses, as well as the implementation of selection criteria, identified 19 critical GPCR genes: *ADGRF1*, *ADORA1*, *ADRB2*, *AGTR1*, *C5AR2*, *CCKBR*, *FFAR1*, *HCAR3*, *HCRTR2*, *HRH2*, *HTR1B*, *LGR4*, *LPAR3*, *MTNR1B*, *NMUR2*, *OXGR1*, *OXTR*, *P2RY12*, and *PRLHR* (Table 1). GPCRs are grouped into six classes (A to F) based on sequence homology and functional similarity (34). Sixteen of 19 GPCR genes were identified as class A; *ADGRF1* belongs to class B, *C5AR2* is a nonclassical GPCR, and *LGR4* is an orphan receptor. To limit off-target results, the 19 GPCR genes identified by SMARTpool screens were reexamined by deconvolution of the siRNA pools (24, 47). Here, A549 cells were transfected with individual ON TARGETplus (OTP)-modified siRNAs from the SMARTpool. OTP-siRNAs have improved gene targeting due to a dual-strand modification that provides increased interaction with the RNA-induced silencing complex (RISC), decreasing off-target effects by antisense strands (48).

OTP-siRNA-transfected A549 cells were infected (MOI, 0.01) with A/WSN/33, and after 48 h, the levels of infectious virus production were determined by a plaque assay. GPCR genes that were knocked down by OTP-siRNAs and had decreases in virus plaque titers for two or more individual OTP-siRNAs were further evaluated. For example, silencing of the *MTNR1B* gene by transfecting cells with siRNA 4 from the SMARTpool markedly reduced influenza virus titers, but transfection of siRNA 1, 2, or 3 had only a modest effect (Fig. 1A); thus, the *MTNR1B* gene was not considered further. Additionally, silencing of the *NMUR2* or *PRLHR* gene had no substantial effect on viral titers (Fig. 1A). In contrast, OTP-siRNA knockdown of the *ADGRF1*, *ADORA1*, *ADRB2*, *AGTR1*, *C5AR2*, *CCKBR*, *FFAR1*, *HCAR3*, *HCRTR2*, *HRH2*, *HTR1B*, *LGR4*, *LPAR3*, *OXGR1*, *OXTR*, or *P2RY12* gene resulted in decreased virus titers (≤ -1.0) for two or

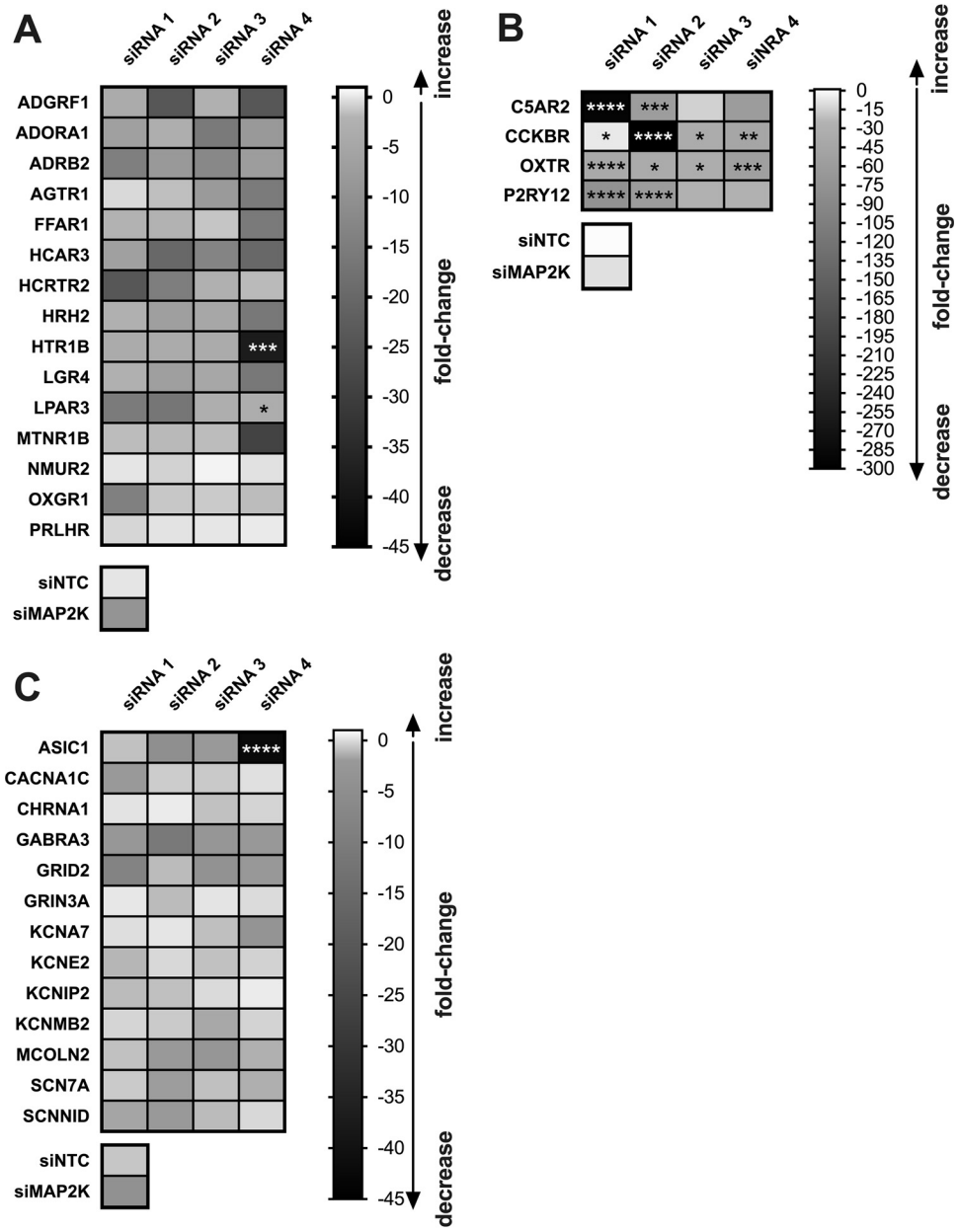

FIG 1 Deconvolution of siRNA pools. siRNA pools targeting GPCR (A, B) and IC (C) genes were deconvoluted and reverse transfected at a final concentration of 50 nM in A549 cells. At 48 h post-siRNA transfection, the A549 cells were infected (MOI, 0.001) with A/WSN/33; supernatants were collected, and virus titers were determined by an MDCK plaque assay. Experiments were performed in triplicate and assayed in duplicate. Results are presented as heat maps depicting fold changes in influenza virus titers (in PFU per milliliter) from titers with a nontargeting control siRNA (siNTC). A positive fold change equates to an increase in PFU per milliliter over the control. A negative fold change equates to a decrease in PFU per milliliter over the control. A zero fold change equates to no change in PFU per milliliter over the control. Asterisks indicate significant differences from the control by two-way mixed analysis of variance with Dunnett's multiple-comparison test (*, $P < 0.05$; **, $P < 0.001$; ***, $P < 0.0001$; ****, $P < 0.00001$). siNTC results are corrected to zero to reflect the baseline change in replication (which is zero). Results are normalized to those for the siNTC control.

more siRNAs (Fig. 1A and B), and knockdown of the *C5AR2*, *CCKBR*, *OXTR*, or *P2RY12* gene gave the greatest reduction in virus titers for two or more siRNAs (Fig. 1B). Knockdown of the *ADGRF1*, *ADRB2*, *C5AR2*, *CCKBR*, *HCRTR2*, *LPAR3*, *OXTR*, or *P2RY12* gene yielded a greater reduction in infectious viral titers than knockdown of the mitogen-activated protein kinase kinase (MAP2K) gene (−9.54-fold change), which is known to limit the replication of influenza virus and thus to reduce infectious viral

TABLE 2 IC genes from a genome-wide RNAi screen

Gene	Function	Z-score[a]
ASIC1	Acid-sensing (proton-gated) ion channel 1	−1.8
CACNA1C	Calcium channel, voltage dependent, L type, alpha 1C subunit	−2.2
CHRNA1	Cholinergic receptor, nicotinic, alpha 1 (muscle)	−1.5
GABRA3	Gamma-aminobutyric acid (GABA) A receptor, alpha 3	−1.5
GRID2	Glutamate receptor, ionotropic, delta 2	−1.8
GRIN3A	Glutamate receptor, ionotropic, *N*-methyl-D-aspartate 3A	−1.5
KCNA7	Potassium voltage-gated channel, shaker-related subfamily, member 7	−1.5
KCNAB2	Potassium voltage-gated channel, shaker-related subfamily, beta member 2	−1.7
KCNE2	Potassium voltage-gated channel, Isk-related family, member 2	−1.4
KCNIP2	Kv channel-interacting protein 2	−1.9
MCOLN2	Mucolipin 2	−1.9
SCN7A	Sodium channel, non-voltage gated 1, delta subunit	−1.5
SCNN1D	Sodium channel, voltage gated, type VII, alpha subunit	−2.0

[a]A negative Z-score indicates a proinfluenza gene.

titers (Fig. 1A and B) (49, 50). Thus, 16 GPCR genes (*ADGRF1*, *ADORA1*, *ADRB2*, *AGTR1*, *C5AR2*, *CCKBR*, *FFAR1*, *HCAR3*, *HCRTR2*, *HRH2*, *HTR1B*, *LGR4*, *LPAR3*, *OXGR1*, *OXTR*, and *P2RY12*) were further evaluated.

An RNAi screen identifies IC genes. Ion channels (ICs) are membrane-spanning proteins that allow for ion flux across cellular membranes (51), which affects signaling cascades and effector functions (52), as well as the activity and stability of viral proteins (53–55). Thus, ion channels affect influenza virus replication (40–42), since influenza viruses attach to the cell membranes during infection and incorporate the membrane into an acidified endosome, triggering conformational changes in HA (56, 57). We screened 352 IC genes for their importance in influenza virus replication and found Z-scores of ≤ -1.0 for 173 IC genes. These proviral genes were analyzed by IPA and GO analyses, yielding 13 IC genes (*ASIC1*, *CACNA1C*, *CHRNA1*, *GABRA3*, *GRID2*, *GRIN3A*, *KCNA7*, *KCNE2*, *KCNIP2*, *KCNMB2*, *MCOLN2*, *SCN7A*, and *SCNN1D*) (Table 2). OTP-siRNA SMARTpools were deconvoluted (1 siRNA pool per treatment; 4 siRNAs per target) and reverse transfected into A549 cells, and then the cells were infected (MOI, 0.01) with A/WSN/33 after 48 h (24, 56). Levels of infectious influenza virus were determined by a plaque assay. IC genes that showed decreased plaque titers for two or more individual OTP-siRNAs were further evaluated. Silencing the *CACNA1C*, *CHRNA1*, *GRIN3A*, *KCNA7*, *KCNE2*, *KCNIP2*, *KCNMB2*, or *SCN7A* gene did not detectably affect virus titers relative to those for nontargeting siRNA controls (siNTC) (Fig. 1C); however, silencing the *ASIC1*, *GABRA3*, *GRID2*, *MCOLN2*, or *SCNN1D* gene resulted in a <-1.0-fold change. Silencing *ASIC1* led to a greater reduction in influenza virus titers than silencing the MAP2K gene (−4.3-fold change). Silencing *SCNN1D* resulted in a small decrease in viral titers; however, since *SCNN1D* is targeted by the ion channel inhibitor triamterene, and thus, a potential repurposed drug, identified by IPA, was available, this gene was further evaluated (58, 60). Thus, a total of five ion channel genes—*ASIC1*, *GABRA3*, *GRID2*, *MCOLN2*, and *SCNN1D*—were further evaluated.

Distinctive GPCR and IC genes are utilized for the replication of influenza virus strains and subtypes. To better understand GPCR and IC genes that have influenza virus strain and type differences, the GPCR and IC genes were evaluated following A/CA/04/2009 or B/Yamagata/16/1988 infection of A549 cells using a plaque assay and a 50% tissue culture infective dose ($TCID_{50}$) assay. Our initial RNAi screen investigated A/WSN/33 infection of A549 cells at a lower MOI (0.001). To corroborate earlier data, gene hits were confirmed using individual OTP-siRNAs and a higher MOI (0.01) of A/WSN/33. The higher MOI of 0.01 was repeated for RNAi silencing of GPCR and IC genes in A549 cells infected with A/CA/04/2009 or B/Yamagata/16/1988. Briefly, A549 cells were transfected with OTP-siRNAs (2 siRNAs per target, transfected individually) targeting a GPCR or ion channel gene selected from the A/WSN/33 deconvolution screen. Following reverse transfection for 48 h, the A549 cells were infected with either A/WSN/33 (MOI, 0.01), A/CA/04/2009 (MOI, 0.1), or B/Yamagata/16/1988 (MOI, 0.1).

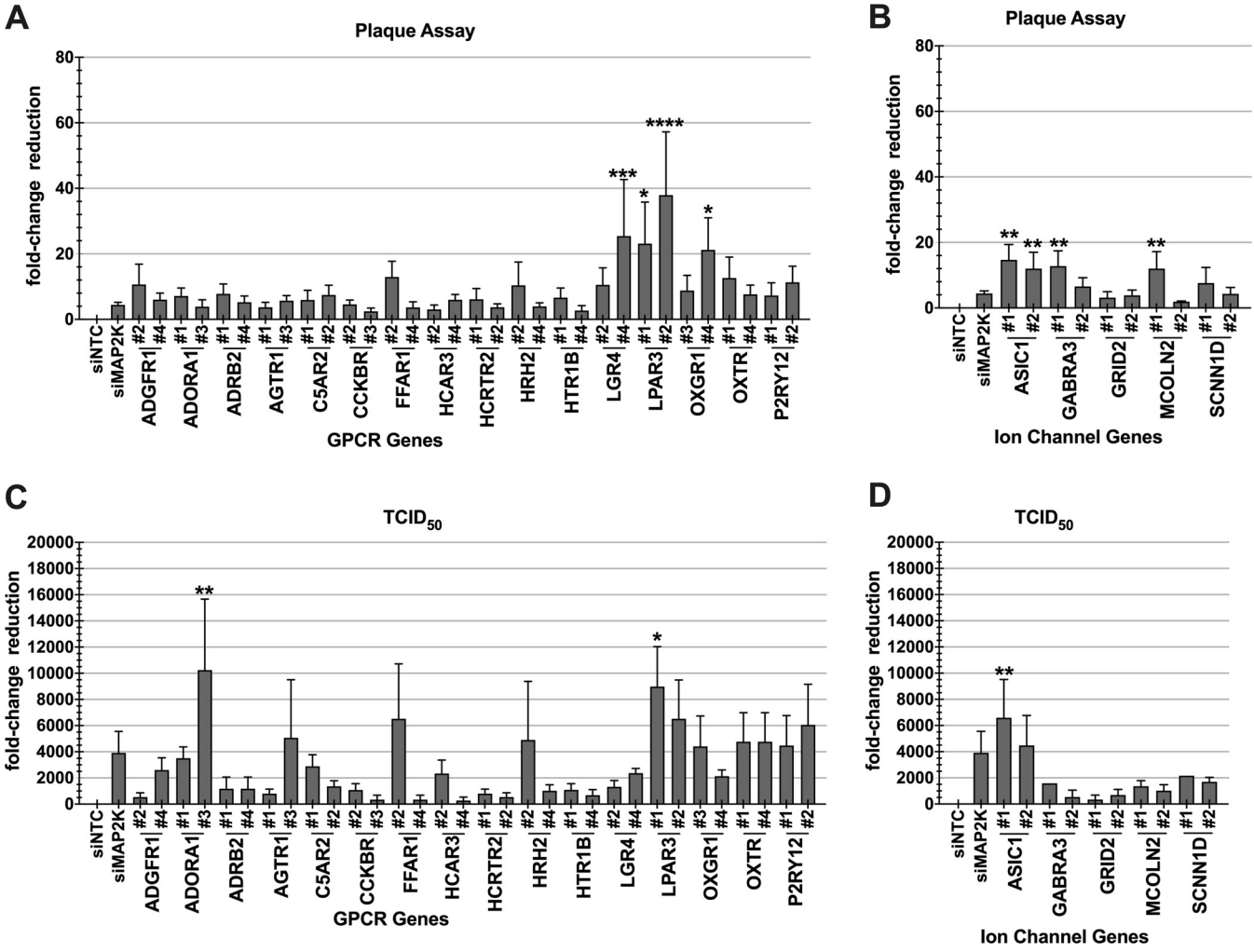

FIG 2 Validation of host gene targets for A/WSN/33-infected A549 cells. A549 cells were reverse transfected (50 nM) with OTP-modified siRNAs (2 siRNAs per gene target) from the deconvolution siRNA screen in triplicate and were incubated for 48 h. The A549 cells were infected (MOI, 0.01) with A/WSN/33. Supernatants were collected 48 h postinfection. Infectious viral titers (expressed as PFU per milliliter) and $TCID_{50}$ titers were determined by an MDCK plaque assay and sample titration on MDCK cells followed by an HA assay, respectively. Plaque assay data for GPCR (A) and ion channel (B) genes and $TCID_{50}$ data for GPCR (C) and ion channel (D) genes are presented as the inverse of the fold decrease from the level with nontargeting control siRNA (siNTC) for three independent experiments performed in triplicate. A positive increase in the fold change equates to a decrease in PFU per milliliter or $TCID_{50}$ per milliliter from that with siNTC. Data show means ± standard errors of the means for three independent experiments performed in triplicate. Asterisks indicate significant differences from the control by ordinary one-way analysis of variance with Dunnett's multiple-comparison test (*, $P < 0.05$; **, $P < 0.001$; ***, $P < 0.0001$; ****, $P < 0.00001$). siNTC results are corrected to zero to reflect the baseline change in replication (which is zero). Results are normalized to those for siNTC. Numbers under graphs represent individual siRNAs from the SMARTpool (siRNA 1, 2, 3, or 4) targeting a particular gene.

Forty-eight hours postinfection, the titer and 50% tissue culture infective dose were determined by a plaque assay and a $TCID_{50}$ HA assay, respectively. The results showed that silencing 16 GPCR and 5 IC proinfluenza genes individually was associated with a >2-fold decrease in influenza plaque formation in A549 cells infected with A/WSN/33 (Fig. 2A and B), A/CA/04/2009 (Fig. 3A and B), or B/Yamagata/16/1988 (Fig. 4A and B). Notably, there was a >100-fold decrease in $TCID_{50}$ for A/WSN/33 (Fig. 2C and D), a >10-fold decrease in $TCID_{50}$ for CA/04/2009 (Fig. 3C and D), and a >10-fold decrease in $TCID_{50}$ for B/Yamagata/16/1988 (Fig. 4C and D). These differences in the fold change are likely related to the virus replication dynamics and growth kinetics. The A/WSN/33 and CA/04/2009 strains replicate at a higher tempo and to higher titers than B/Yamagata/16/1988 (52, 53). As shown in Fig. 2, siRNA silencing of the *LGR4*, *LPAR3*, *OXGR1*, *ASIC1*, *GABRA3*, or *MCOLN2* gene markedly reduced A/WSN/33 virus titers from those with siNTC while also showing a reduction in virus titers from those with siMAP2K (4.4-fold decrease) (Fig. 2A and B). The effects of individually silencing the 16

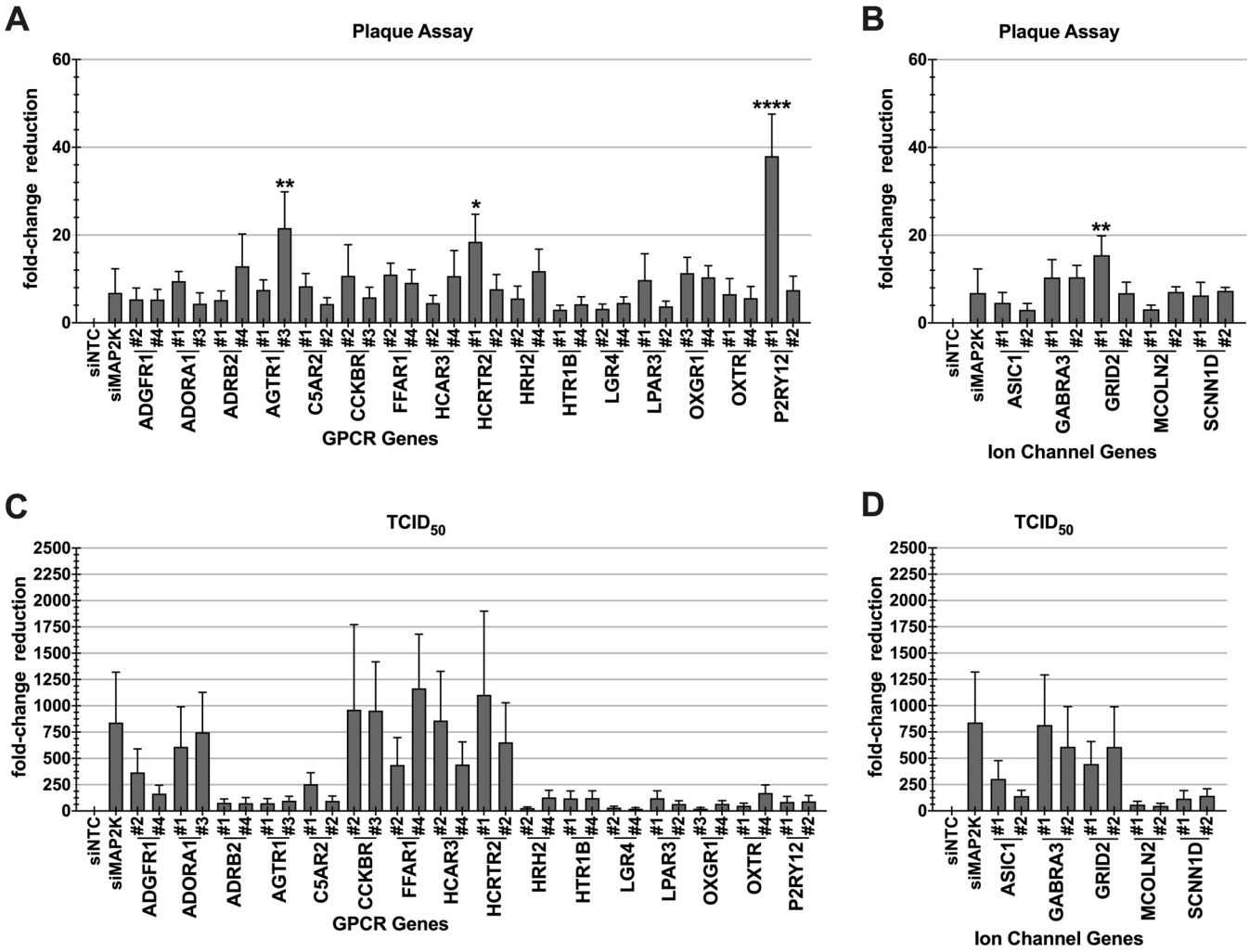

FIG 3 Validation of host gene targets for A/CA/04/2009-infected A549 cells. A549 cells were reverse transfected (50 nM) with OTP-modified siRNAs (2 siRNAs per gene target) from the deconvolution siRNA screen in triplicate and were incubated for 48 h. The A549 cells were infected (MOI, 0.01) with A/CA/04/09. Supernatants were collected 48 h postinfection. Infectious viral titers (expressed as PFU per milliliter) and $TCID_{50}$ titers were determined by an MDCK plaque assay and sample titration on MDCK cells followed by an HA assay, respectively. Plaque assay data for GPCR (A) and ion channel (B) genes and $TCID_{50}$ data for GPCR (C) and ion channel (D) genes are presented as the inverse of the fold decrease from the level with nontargeting control siRNA (siNTC) for three independent experiments performed in triplicate. A positive increase in the fold change equates to a decrease in PFU per milliliter or $TCID_{50}$ per milliliter from that with siNTC. Data show means ± standard errors of the means from three independent experiments performed in triplicate. Asterisks indicate significant differences from the control by ordinary one-way analysis of variance with Dunnett's multiple-comparison test (*, $P < 0.05$; **, $P < 0.001$; ***, $P < 0.0001$; ****, $P < 0.00001$). siNTC results are corrected to zero to reflect the baseline change in replication (which is zero). Results are normalized to those with siNTC. Numbers under graphs represent individual siRNAs from the SMARTpool (siRNA 1, 2, 3, or 4) targeting a particular gene.

GPCR and 5 IC genes on A/CA/04/2009 replication were also determined (Fig. 3). The results show that siRNAs targeting the *AGTR1*, *HCRTR2*, *P2RY12*, or *GRID2* gene substantially reduced A/CA/04/2009 replication (Fig. 3A and B). Silencing *P2RY12* also showed a considerable reduction in virus titers from those with siMAP2K (6.84-fold reduction) (Fig. 3A). The result of individually silencing 16 GPCR genes and 5 IC genes on B/Yamagata/16/1988 replication was also determined (Fig. 4). Importantly, silencing the *HRH2* or *GRID2* gene substantially reduced the B/Yamagata/16/1988 titer, and targeting *HRH2* resulted in a reduction in the virus titer greater than that with siMAP2K (30-fold reduction) gene silencing (Fig. 4A and B). These results confirm earlier results from the A/WSN/33 screen and show that several GPCR and IC genes affect A/CA/04/09 and B/Yamagata/16/1988 replication.

DISCUSSION

RNAi screens have aided in the discovery of essential features of the host-virus

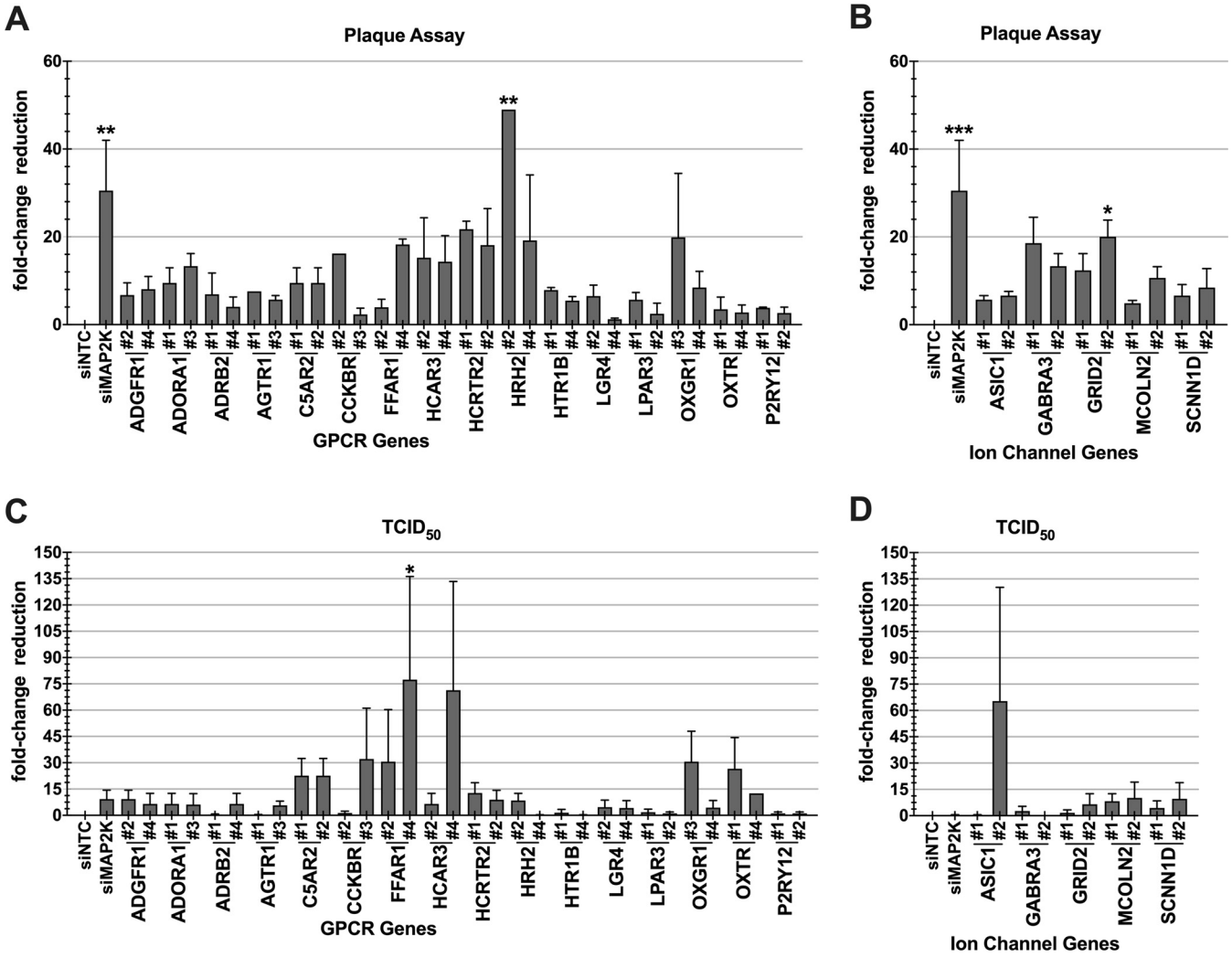

FIG 4 Validation of host gene targets for B/Yamagata/16/1988-infected A549 cells. A549 cells were reverse transfected (50 nM) with OTP-modified siRNAs (2 siRNAs per gene target) from the deconvolution siRNA screen in triplicate and were incubated for 48 h. The A549 cells were infected (MOI, 0.01) with B/Yamagata/16/1988. Supernatants were collected 48 h postinfection. Infectious viral titers (PFU per milliliter) and $TCID_{50}$ titers were determined by an MDCK plaque assay and sample titration on MDCK cells followed by an HA assay, respectively. Plaque assay data for GPCR (A) and ion channel (B) genes and $TCID_{50}$ data for GPCR (C) and ion channel (D) genes are presented as the inverse of the fold decrease from the level with nontargeting control siRNA (siNTC) for three independent experiments performed in triplicate. A positive increase in the fold change equates to a decrease in PFU per milliliter or $TCID_{50}$ per milliliter from that with siNTC. Data show means ± standard errors of the means for three independent experiments performed in triplicate. Asterisks indicate significant differences from the control by ordinary one-way analysis of variance with Dunnett's multiple-comparison test (*, $P < 0.05$; **, $P < 0.001$; ***, $P < 0.0001$; ****, $P < 0.00001$). siNTC results are corrected to zero to reflect the baseline change in replication (which is zero). Results are normalized to those for siNTC. Numbers under graphs represent individual siRNAs from the SMARTpool (siRNA 1, 2, 3, or 4) targeting a particular gene.

interface, specifically the host pathways used to facilitate virus replication (23, 54), and have provided information used to develop disease intervention strategies (28, 29). GPCRs and ICs are implicated in the replication mechanisms of several RNA viruses, including severe acute respiratory syndrome coronavirus 2 (SARS-CoV-2), Marburg virus, Ebola virus, and HIV, but have not been well described for influenza virus (38, 40, 41, 46, 55). In this study, we identified GPCR and IC genes used by influenza virus for replication and determined influenza virus strain and type differences. We screened 390 GPCR and 349 IC genes, of which 19 GPCR and 13 IC genes were selected for validation studies. Secondary validation by siRNA pool deconvolution yielded 16 confirmed GPCR genes (*ADGRF1*, *ADORA1*, *ADRB2*, *AGTR1*, *C5AR2*, *CCKBR*, *FFAR1*, *HCAR3*, *HCRTR2*, *HRH2*, *HTR1B*, *LGR4*, *LPAR3*, *OXGR1*, *OXTR*, and *P2RY12*) and 5 IC genes (*ASIC1*, *GABRA3*, *GRID2*, *MCOLN2*, and *SCNN1D*) (Fig. 1). The genes from the RNAi screen were validated by using two individual OTP-siRNAs and testing the effects on A/WSN/33

replication using a higher MOI (0.01) to ensure robust infection. These studies used two endpoints to evaluate the effects of knockdown on influenza virus replication: infectious virus titers (expressed in PFU per milliliter), quantitated by plaque assays, and the amount of virus required to infect 50% of cells (50% tissue culture infective dose [$TCID_{50}$]), measured by HA assays (Fig. 2). siRNA silencing of GPCR genes *LGR4*, *LPAR3*, and *OXGR1*, and silencing of IC genes *ASIC1*, *GABRA3*, and *MCOLN2*, in A549 cells yielded substantial decreases in A/WSN/33 titers, showing that these genes are needed for A/WSN/33 replication. Of note, the decreases in virus plaque numbers were greater than those with the control siRNA siMAP2K (4-fold decrease), which targets mitogen-activated protein kinase, shown to be required for influenza virus replication (49, 50).

To examine influenza virus strain differences, siRNA-transfected A549 cells were infected with A/CA/04/2009, a representative circulating strain of human influenza A virus, and levels of virus replication were determined by quantification of infectious virus (by plaque assay) and determination of the $TCID_{50}$ following transfection (Fig. 3). Silencing of GPCR and IC genes gave results similar to those for A/WSN/33-infected A549 cells, where influenza virus titers linked to the GPCR genes *AGTR1*, *HCRTR2*, and *P2RY12* and the IC gene *GRID2* were considerably reduced. Of note, silencing *P2RY12* reduced virus titers 6-fold more than the siMAP2K control. We also examined the potential for influenza virus type differences linked to GPCR and IC genes in A549 cells by evaluating the replication of B/Yamagata/16/1988 after siRNA transfection (Fig. 4). siRNA silencing of GPCR and IC genes also yielded reduced B/Yamagata/16/1988 replication, but the reductions were statistically significant ($P < 0.01$) only for the *HRH2* and *GRID2* genes; targeting *HRH2* yielded a reduction in virus titers greater than that with siMAP2K (30-fold change).

The results suggest that influenza virus strains and types coopt similar GPCR and IC genes as part of the replication process in A549 cells but have the ability to utilize different genes in similar pathways (54, 61). It has been reported that the tempo of signal transduction and host gene expression is associated with viral replication and virus production dynamics (61). It is possible that different host genes are used for influenza virus replication in other cell types, particularly since transformed cell lines can have distinct gene expression (62). This is a caveat with A549 cells, since some host genes identified as important may not translate to primary cell cultures. Additionally, the findings in this study were limited to 48 h postinfection (p.i.) due to the high-throughput screening procedure, and the later phases of virus replication were not evaluated. Additionally, GPCR signaling is a complex network; each GPCR complex may have a number of isoforms and splice variants that create hundreds of combinations of G proteins. Thus, differences in cell signaling associated with the kinetics of infection and/or GPCR isoforms/splice variants can go unnoticed (34). In addition, the configuration of the G protein affects not only which transmembrane receptor it can bind to but also which downstream target is affected (34, 63, 64). GPCR $G\alpha$ subunits are grouped into four families ($G\alpha_s$, $G\alpha_i$, $G\alpha_q$, and $G\alpha_{12/13}$) based on sequence homology, consisting of approximately 20 distinct $G\alpha$ subunit proteins due to splice variants (65). The host genes *ADORA1*, *AGTR1*, *HTR1B*, and *P2RY12* are coupled to $G\alpha_i$ (Fig. 5), while the *ADRB2*, *HCAR3*, and *HRH2* genes are coupled to $G\alpha_s$ (Fig. 6). $G\alpha_i$ signaling inhibits adenyl cyclase, which decreases intracellular cAMP levels, while $G\alpha_s$ signaling stimulates adenyl cyclase, prompting the opposing effect. Modulation of cAMP levels regulates the duration and intensity of cAMP signaling via feedback mechanisms (66). G proteins have been implicated in late stages of influenza virus infection, specifically virus budding (67–69). The host genes *AGTR1*, *CCKBR*, *FFAR1*, *HCRTR2*, *OXGR1*, and *OXTR* were associated with $G\alpha_q$ signaling by IPA (Fig. 7). $G\alpha_q$ signaling is associated with multiple downstream pathways, but the best characterized are those associated with phospholipase $C\beta$ (PLC) activation and phosphatidylinositol 3-kinase (PI3K) (70). Alteration of this pathway has been shown to play a regulatory role in the clathrin-mediated and clathrin-independent endocytosis pathways utilized by influenza virus at entry (71). The host genes *ADGRF1* and *LGR4* are orphan receptors, with no identified endogenous

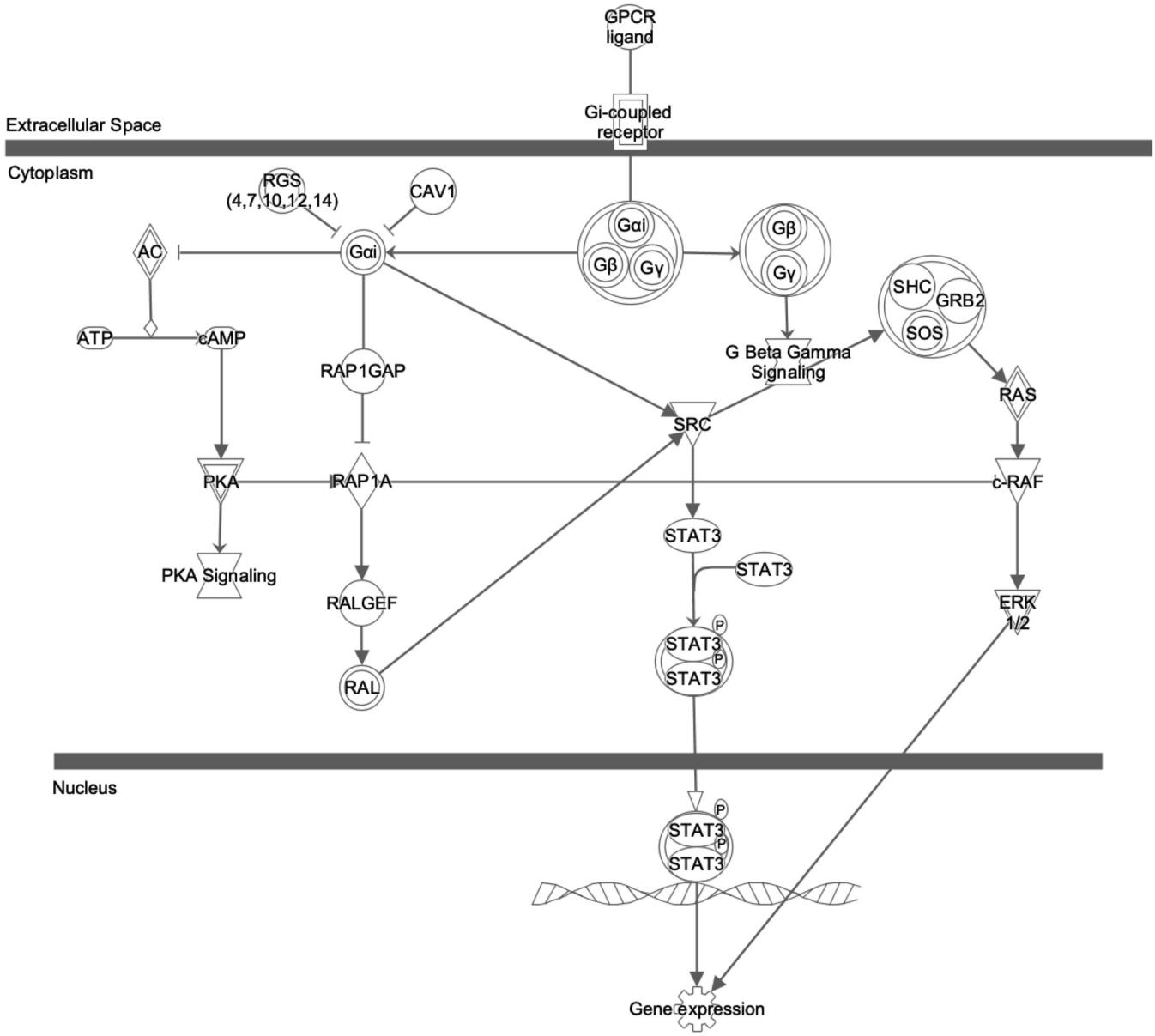

FIG 5 Gα_i signaling pathway generated by IPA. The *ADORA1*, *AGTR1*, *HTR1B*, and *PYR12* genes were associated with Gα_i signaling by IPA. AC, adenylyl cyclase; cAMP, cyclic AMP; PKA, protein kinase A; RGS, regulators of G protein signaling; CAV1, Caveolin-1; RAP1GAP, RAP1 GTPase-activating protein; RAP1A, Ras-related protein Rap-1A; RALGEF, Ras-like small GTPase; RAL, Ras-like protein; SRC, Src protein kinase; STAT3, signal transducer and activator of transcription 3; GRB2, growth factor receptor-bound protein 2; SHC, adaptor protein; SOS, guanine nucleotide exchange protein; c-RAF, RAF proto-oncogene serine/threonine-protein kinase; ERK 1/2, extracellular signal-regulated kinase.

ligand (72–74). C5AR2 is a nonclassical GPCR, and although it is a seven-transmembrane receptor, it does not couple to a G protein and instead binds β-arrestins (75, 76). In this study, we show that siRNA silencing of the GPCR genes *AGTR1*, *CCKBR*, *FFAR1*, *HCRTR2*, *OXGR1*, and *OXTR* inhibits A/WSN/33, A/CA/04/2009, and B/Yamagata/16/1988 replication in A549 cells.

IPA of the validated IC genes determined in this study suggested that several genes affected influenza virus replication. *ASIC1* is an acid-sensing sodium channel gene whose regulation is controlled by activation of the PKC pathway (77); however, it remains unclear how *ASIC1* is necessary for viral replication. Similarly, *GRID2* (or *GluRδ2*) is an orphan glutamate receptor gene whose function is poorly understood (78). SCNN1D (the delta subunit of the epithelial sodium channel [δENaC]) is one of four subunits that compose the epithelial sodium channel located on the apical

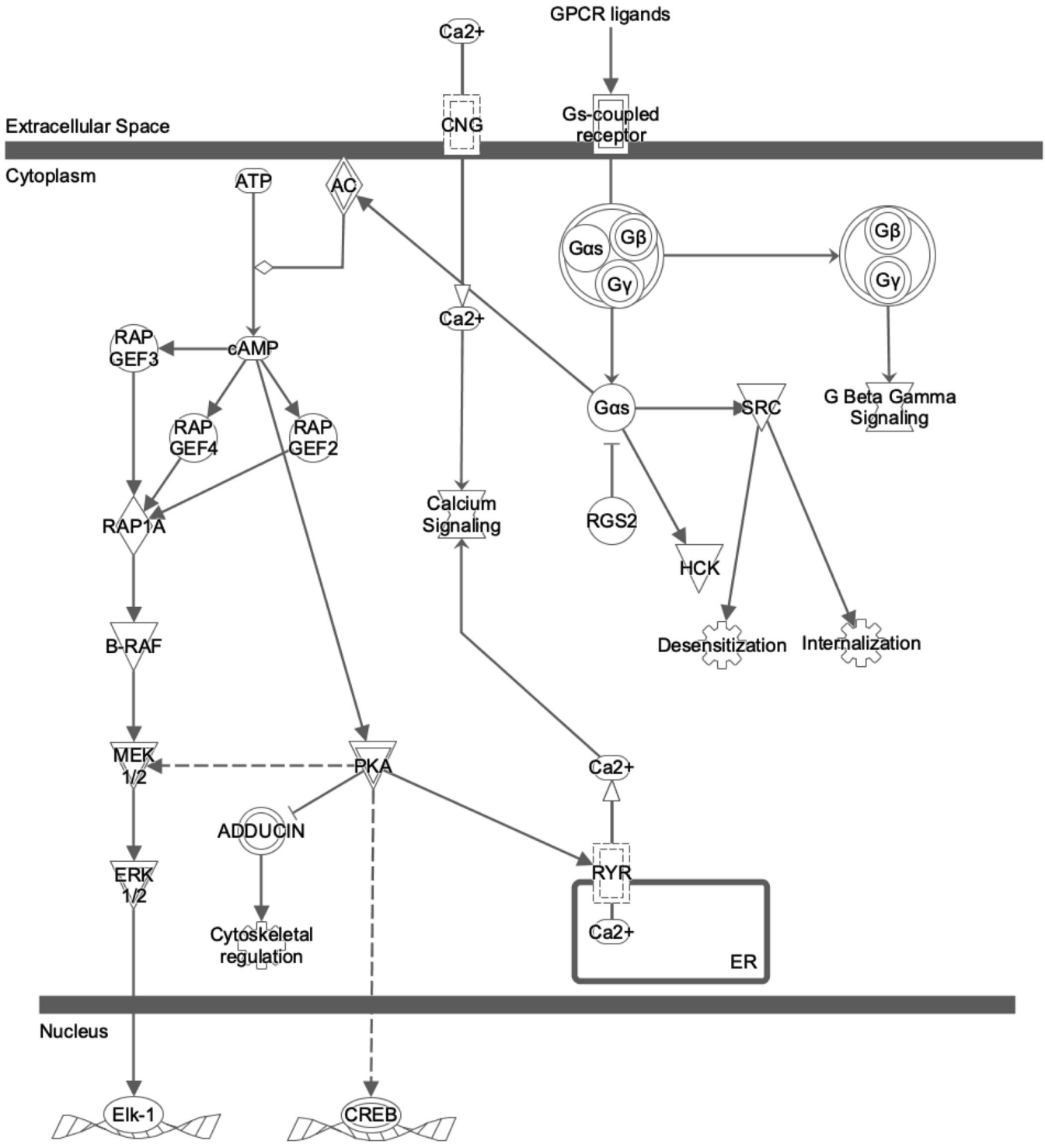

FIG 6 Gα_s signaling pathway generated by IPA. The *ADRB2*, *HCAR3*, and *HRH2* genes were associated with Gα_s signaling by IPA. AC, adenylyl cyclase; cAMP, cyclic AMP; PKA, protein kinase A; RGS2, regulators of G protein signaling; RAP1A, Ras-related protein Rap-1A; RAPGEF 2, 3, and 4, Rap guanine nucleotide exchange factors 2, 3, and 4; SRC, Src protein kinase; B-RAF, RAF proto-oncogene serine/threonine-protein kinase; MEK 1/2, mitogen-activated kinases 1 and 2; ERK 1/2, extracellular signal-regulated kinases 1 and 2; CNG, cyclic-nucleotide-gated ion channel; HCK, tyrosine protein kinase; RYR, ryanodine receptor; ER, endoplasmic reticulum; CREB, cAMP response element-binding protein; Elk-1, ETS-like-1 protein.

surfaces of polarized tissues, e.g., the lung. It is involved in Na^+ transport across the transepithelial surface during Na^+ reabsorption (60, 79). In this study, silencing of *SCNN1D* reduced virus replication, suggesting a novel role for this subunit compared to its α, β, and γ counterparts (80). GABRA3 has been shown to be expressed in the

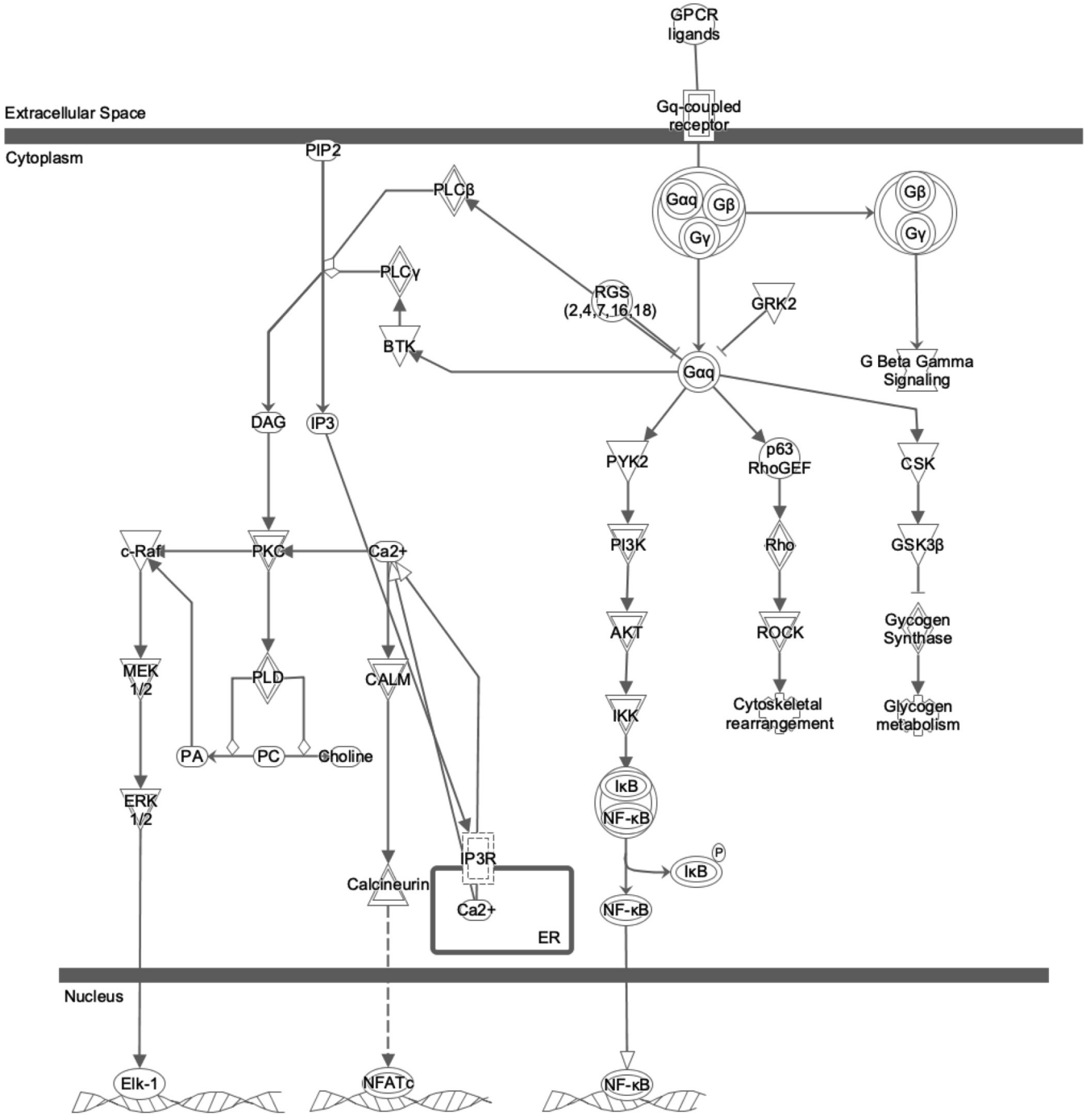

FIG 7 Gα_q signaling pathway generated by IPA. The *AGTR1*, *CCKBR*, *FFAR1*, *HCRTR2*, *OXGR1*, and *OXTR* genes were associated with Gα_q signaling. RGS, regulators of G protein signaling; c-RAF, RAF proto-oncogene serine/threonine-protein kinase; MEK 1/2, mitogen-activated kinases 1 and 2; ERK 1/2, extracellular signal-regulated kinase; PIP2, phosphatidylinositol biphosphate; IP3, inositol triphosphate; DAG, diacylglycerol; PKC, protein kinase C; PLD, phospholipase D; PA, phosphatidic acidic; PC, phosphatidylcholine; CALM, clathrin assembly lymphoid myeloid leukemia protein; NFATc, nuclear factor-activated T cells, cytoplasmic; PYK2, Tau tyrosine kinase; PI3K, phosphatidylinositol 3-kinase; AKT, protein kinase B; IKK, IκB kinase; NF-κB, nuclear factor kappa-light-chain enhancer of activated B cells; RhoGEF, Rho guanine nucleotide exchange factor; ROCK, Rho-associated protein kinase; CSK, tyrosine protein kinase; GSK3β, glycogen synthase kinase-3β; PLCβ, phospholipase Cβ; BTK, Bruton tyrosine kinase.

lung (81), and its activation is linked to autophagy (81), a strategy used by influenza viruses to promote replication (82). We show that *GABRA3* silencing reduces viral replication. It has been shown that MCOLN2 is associated with improved influenza virus, dengue virus, yellow fever virus, and equine arteritis virus infectivity (83), possibly by promoting virus trafficking between the early and late endosomes and releasing virus

TABLE 3 Summary of FDA-approved drugs that target proinfluenza GPCR and ion channel genes

Target	Drug name	PubChem ID	CAS no.	Action	Chemical formula	Reference(s)
ADORA1	Aminophylline	9433	317-34-0	Antagonist	$C_{16}H_{24}N_{10}O_4$	98
	Dyphylline	3182	479-18-5	Antagonist	$C_{10}H_{14}N_4O_4$	98
	Istradefylline	5311037	155270-99-8	Antagonist	$C_{20}H_{24}N_4O_4$	98
	Pentoxifylline	4740	6493-05-6	Unknown	$C_{13}H_{18}N_4O_3$	99, 100
	Theophylline	2153	58-55-9	Antagonist	$C_7H_8N_4O_2$	98
AGTR1	Azilsartan	135415867	147403-03-0	Antagonist	$C_{25}H_{20}N_4O_5$	101, 102
	Candesartan	2541	139481-59-7	Antagonist	$C_{24}H_{20}N_6O_3$	87, 102, 103
	Eprosartan	5281037	133040-01-4	Antagonist	$C_{23}H_{24}N_2O_4S$	102
	Irbesartan	3749	138402-11-6	Antagonist	$C_{25}H_{28}N_6O$	102, 104, 105
	Losartan	3961	114798-26-4	Antagonist	$C_{22}H_{23}ClN_6O$	102
	Valsartan	60846	137862-53-4	Antagonist	$C_{24}H_{29}N_5O_3$	102, 106
HTR1B	Asenapine	3036780	65576-45-6	Antagonist	$C_{17}H_{16}ClNO$	107
P2RY12	Cangrelor	9854012	163706-06-7	Inhibitor	$C_{17}H_{25}Cl_2F_3N_5O_{12}P_3S_2$	108
	Clopidogrel	60606	113665-84-2	Antagonist	$C_{16}H_{16}ClNO_2S$	84–86, 102, 109–111
	Prasugrel	6918456	150322-43-3	Antagonist	$C_{20}H_{20}FNO_3S$	102, 109, 112
	Ticagrelor	9871419	274693-27-5	Inhibitor	$C_{23}H_{28}F_2N_6O_4S$	113
	Ticlopidine	5472	55142-85-3	Antagonist	$C_{14}H_{14}ClNS$	86, 102, 109, 110
ADRB2	Carteolol HCl	40127	51781-21-6	Antagonist	$C_{16}H_{25}ClN_2O_3$	114
	Labetalol	3869	36894-69-6	Antagonist	$C_{19}H_{24}N_2O_3$	102
	Levobunolol	39468	47141-42-4	Antagonist	$C_{17}H_{25}NO_3$	102, 115
	Metipranolol	31477	22664-55-7	Antagonist	$C_{17}H_{27}NO_4$	58, 116
	Sotalol	5253	3930-20-9	Antagonist	$C_{12}H_{20}N_2O_3S$	117
	Timolol	33624	26839-75-8	Antagonist	$C_{13}H_{24}N_4O_3S$	118
HRH2	Asenapine	3036780	65576-45-6	Antagonist	$C_{17}H_{16}ClNO$	107
	Famotidine	5702160	76824-35-6	Antagonist	$C_8H_{15}N_7O_2S_3$	119
	Lafutidine	5282136	118288-08-7	Antagonist	$C_{22}H_{29}N_3O_4S$	120
ASIC1	Amiloride	16231	2609-46-3	Inhibitor	$C_6H_8ClN_7O$	90
	Diclofenac	3033	15307-86-5	Inhibitor	$C_{14}H_{11}Cl_2NO_2$	121
GABRA3	Bicuculline	10237	485-49-4	Antagonist	$C_{20}H_{17}NO_6$	122
OXTR	Atosiban	5311010	90779-69-4	Antagonist	$C_{43}H_{67}N_{11}O_{12}S_2$	123, 124
SCNN1D	Amiloride	16231	2609-46-3	Inhibitor	$C_6H_8ClN_7O$	125
	Triamterene	5546	396-01-0	Inhibitor	$C_{12}H_{11}N_7$	58, 116, 126

into the cytosol independently of interferon (IFN) signaling (83). Our findings concur, showing that siRNA silencing of *MCOLN2* decreases influenza virus replication and that MCOLN2 is an important host factor not only for the replication of IAVs but also for that of IBVs, which was not previously known.

Understanding the host factors used by influenza virus during entry, replication, and egress can help identify targets for drug repurposing or for the development of novel antiviral drugs. Targeting of host factors is refractory to the development of drug resistance generated by viral mutations (18). Here, we identify several GPCR and ion channel genes that can be targeted by FDA-approved drug antagonists and/or inhibitors (Table 3). For example, *P2RY12* (a GPCR gene) can be targeted by the drug clopidogrel bisulfate (Plavix), which is currently approved for the inhibition of platelet aggregation and the treatment of patients with acute coronary syndrome (84–86). Interestingly, the *AGTR1* gene (a GPCR gene) has been shown to be associated with the coronavirus infection pathway, which has a possible link between angiotensin-converting enzyme 2 (ACE2) and lung injury (127–129). *AGTR1* can be targeted by angiotensin receptor blockers (ARBs), including candesartan, which has been suggested as a treatment for coronavirus disease 2019 (COVID-19) (87). ARBs have shown efficacy in decreasing lung injury in animal models of acute respiratory distress syndrome (ARDS), but not without potential side effects (88). Further studies are needed to determine the importance of this association with COVID-19. The ion channels ASIC1 and

SCNN1D can be inhibited by amiloride, which has been shown to suppress the replication of coxsackievirus B3 (CVB3) and foot-and-mouth disease virus (FMDV) (89, 90). These examples show the therapeutic potential of drug repurposing to target host factors needed for virus replication.

To summarize, this study identified and evaluated GPCR and IC genes coopted by influenza viruses (A/WSN/33, CA/04/2009, B/Yamagata/16/1988) for replication and identified strain and type differences. Collectively, the identification of these GPCR and IC genes provides the opportunity to develop host-directed virus control strategies to limit influenza virus replication and disease using drug repurposing or the development of novel antivirals.

MATERIALS AND METHODS

Cells and viruses. Type II human lung epithelial (A549) cells (ATCC CCL-185) were propagated in Dulbecco's modified Eagle's medium (DMEM; HyClone, Logan, UT) supplemented with 5% heat-inactivated fetal bovine serum (HI-FBS; Atlas Biologics Inc., Fort Collins, CO). Madin-Darby canine kidney (MDCK) cells (ATCC CCL-34) were propagated in DMEM supplemented with 5% HI-FBS. All experiments were performed using log-phase A549 or MDCK cells.

A/WSN/33 (H1N1; ATCC VR-825), which is lab adapted and trypsin independent (38, 39), A/CA/04/2009 (H1N1; BEI Resources), and B/Yamagata/16/1988 (BEI Resources) were grown in 9-day-old embryonated chicken eggs as described previously (91). The A/WSN/33 and A/CA/04/2009 viruses used in siRNA validation and miR studies were propagated in MDCK cells (91). Viral titers were determined by plaque assays and were calculated using the Reed and Muench method (92–94).

siGENOME screen. siGENOME plates received from Dharmacon/Horizon Discovery were preloaded with 0.5 nmol of pooled, lyophilized siRNAs targeting 390 GPCR or 349 IC genes. siRNAs were designed to ensure ≥85% knockdown of target gene expression, and optimal antisense-strand RISC loading is guaranteed (95). siRNA pools were resuspended in siRNA resuspension buffer to a concentration of 1 μM, aliquoted, and stored at −80°C until use. For the screen, A549 cells were reverse transfected with siRNA SMARTpools or siRNA controls (50 nM) and were incubated at 37°C under 5% CO_2 for 48 h to allow for silencing of the targeted gene prior to virus infection as described previously (24, 30). Briefly, transfections were performed in a 96-well plate format in triplicate. The siRNA SMARTpools were diluted in Hanks' balanced salt solution (HBSS; GIBCO), added to the plate, and incubated at room temperature (RT) for 5 min. Following incubation, 0.4 μl of DharmaFECT 1 transfection reagent (Horizon Discovery) and 9.6 μl of HBSS per well were added, and the mixture was incubated for 20 min at RT. Lastly, 80 μl containing 1.5×10^4 A549 cells in DMEM supplemented with 5% HI-FBS was added to each well, and the mixture was incubated at 37°C under 5% CO_2 for 48 h. After transfection, the cells were washed twice with phosphate-buffered saline (PBS), infected with A/WSN/33 at an MOI of 0.001 to reduce defective interfering particles, and incubated at 37°C under 5% CO_2 for 48 h. After infection, the supernatant was collected and analyzed by a $TCID_{50}$ assay for virus replication by HA titers as described previously (24). HA titer results were normalized to those with siNTC. A primary screen was performed twice in two independent experiments. Results were pooled and analyzed. All RNA interference (RNAi) experiments were completed according to the Minimum Information about an RNAi Experiment (MIARE) guidelines (96).

Host genes with a Z-score of ≤−1.0 were considered proinfluenza because siRNA silencing reduced virus replication from that with nontargeting controls. A total of 185 GPCR genes and 173 IC genes were proinfluenza genes (94). These genes were evaluated by Ingenuity Pathway Analysis (IPA; Ingenuity Systems, Inc., Redwood City, CA) and Gene Ontology (GO) analysis. Comprehensive gene interaction networks were determined by combining IPA and GO analysis to identify relationships, functions, mechanisms, and pathways. Following IPA and GO analysis, the GPCR and IC host genes identified were evaluated for their abilities to be targeted by miRs. These data were used to select 19 proinfluenza GPCR and 13 proinfluenza ion channel candidates for further examination.

siRNA pool deconvolution and validation. The four siRNAs per SMARTpool were individually examined in a deconvolution assay to eliminate false-positive results and to determine the most effective siRNAs for reducing influenza virus replication. Plates containing 0.5 nmol of individual lyophilized ON-TARGETplus (OTP) siRNAs (Horizon Discovery) against a single host gene target were tested. OTP-modified siRNAs contained a modification within seed regions to reduce off-target effects and to increase selectivity and effectiveness. siRNAs were suspended in siRNA buffer according to the manufacturer's recommendations to a concentration of 1 μM, aliquoted, and stored at −80°C until use.

A549 cells were reverse transfected with one of four OTP-siRNAs as described elsewhere (44). Briefly, siRNAs targeting a given GPCR or IC gene (Table 4), nontargeting control siRNA (siNTC), siMAP2K (siRNA targeting the mitogen-activated protein kinase 1 gene), or the RNAi transfection control siTOX was used at a final concentration of 50 nM, and transfected cells were incubated at 37°C under 5% CO_2 for 48 h to allow for gene silencing prior to infection. Transfections were performed in a 96-well plate in triplicate. Briefly, siRNA reverse transfection was done using 0.4% DharmaFECT 1 transfection reagent, where siRNA was preincubated with DharmaFECT 1 in serum-free DMEM at RT for 20 min. A549 cells were suspended in DMEM supplemented with 5% HI-FBS, and 1.5×10^4 cells were added to each well. Transfection plates were incubated at 37°C under 5% CO_2 for 48 h. After transfection, the medium was decanted, and the cells were washed twice with PBS and then infected with A/WSN/33 (MOI, 0.001) diluted in infection medium (MEM plus 0.3% bovine serum albumin [BSA] plus 1 μg/ml L-(tosylamido-2-

TABLE 4 Summary of siRNA information for deconvolution experiments[a]

siRNA no.	Gene designation	Gene ID	GenBank accession no.	Target sequence
si1	*ADGRF1*	266977	NM_025048	CACAUGGGCUAAUUAGAAU
si2				CUAUAGAGAUUCCAAGGAG
si3				GUGAAUGUCAUCUCAACAA
si4				GGAGUGCUGUGGCUCAUUU
si1	*ADORA1*	134	NM_000674	AGAGAGGCCUGAUGACUAG
si2				GGAACAAUCUGAGUGCGGU
si3				CCACAGACCUACUUCCACA
si4				CAAGAUCCCUCUCCGGUAC
si1	*ADRB2*	154	NM_000024	UGAUCAUGGUCUUCGUCUA
si2				GGGCAUGGACUCCGCAGAU
si3				CGUCCUGGCCAUCGUGUUU
si4				UUGCCAAGUUCGAGCGUCU
si1	*AGTR1*	185	NM_032049	UGGAAGGCAUAAUUACAUA
si2				CCUGUACGCUAGUGUGUUU
si3				GAAUACCGCUGGCCCUUUG
si4				AUACGUGACUGUAGAAUUG
si1	*C5AR2*	27202	NM_018485	GGAACGAUUCUGUCAGCUA
si2				ACGAAAGUGUGGACAGCAA
si3				UGCAGUGUGUGGUGGACUA
si4				GACCAUGUAUGCCAGCGUC
si1	*CCKBR*	887	NM_176875	GUGAGUGUGUCCACGCUAA
si2				GAAUGUUGCUGGUGAUCGU
si3				GAAUCACUCUUUACGCAGU
si4				GAUGAGCGUUGGAGGAAAU
si1	*FFAR1*	2864	NM_005303	CGCUCAACGUCCUGGCCAU
si2				CCUACAACGCCUCCAACGU
si3				GUGACCGGUUACUUGGGAA
si4				UUCCGGAGGCCGUGCUAUU
si1	*HCAR3*	8843	NM_006018	UCAAAUAACCAUUCCAAGA
si2				AGAAGUUGCUGAUCCAGAA
si3				CGUUCGUGAUGGACUACUA
si4				CGCCAGGGCAGCAUCAUAU
si1	*HCRTR2*	3062	NM_001526	GGUGUUGGCUUAUCUGCAA
si2				CUGCGAAUCCAAUUAUUUA
si3				GGAGCUGAAUGAAACUCAA
si4				UGUCACCCUUUGAUGUUUA
si1	*HRH2*	3274	NM_022304	CCAAGAGGAUCAAUCACAU
si2				GCAAUGUGGUCGUCUGUCU
si3				GUGCAAAGUCCAGGUCAAU
si4				UCAAUGAGGUGUUAGAAGC
si1	*HTR1B*	3351	NM_000863	GGAAAGUACUGCUGGUUAU
si2				GAAUCCGGAUCUCCUGUGU
si3				UCUAUUAACUCGCGGGUUC
si4				GAGCCCAGCUGAUAACCGA
si1	*LGR4*	55366	NM_018490	AGGAUUCACUGUAACGUUA
si2				UUACUGAAGCGACGUGUUA
si3				UAACAACAUUUGCAUCUUG
si4				GCCAAUAACUAACCUAGAU
si1	*LPAR3*	23566	NM_012152	GGACACCCAUGAAGCUAAU
si2				UCUACUACCUGUUGGCUAA
si3				CAACACUGAUACUGUCGAU
si4				UCAUCAUGGUUGUGGUGUA
si1	*MTNR1B*	4544	NM_005959	GCUACUUACUGGCUUAUUU
si2				GUACGACCCACGCAUCUAU
si3				GGUAAUUUGUUCUUGGUGA
si4				GAGAACGGCUCCUUCGCCA
si1	*NMUR2*	56923	NM_020167	CCAUGUGGAUCUACAAUUU
si2				GGUGUCAGGUGUCUUCUUC
si3				UGAAGGGAAUGCAAAUAUU
si4				GGAGCUGACCGAAGAUAUA

(Continued on next page)

TABLE 4 (Continued)

siRNA no.	Gene designation	Gene ID	GenBank accession no.	Target sequence
si1	*OXGR1*	27199	NM_080818	CGGAUGAACUCAAUACUAU
si2				CAUCGUUUCUAGACCAUUA
si3				CCGAUGACCUUCUUGAUCA
si4				CCACUAGACUAUUUAGCAA
si1	*OXTR*	5021	NM_000916	GGAUCACGCUAGCUGUCUA
si2				UGGCAGAACUUGCGGCUCA
si3				GCGUCAAGCUCAUCUCCAA
si4				GAGCAACUCGUCCUCCUUU
si1	P2RY12	64805	NM_176876	GGUCUAGUCUGGCAUGAAA
si2				GUACCGGUCAUACGUAAGA
si3				CAAGUUACCUCCGUCAUAU
si4				CAAGUCAUUUUCUGGAUUA
si1	*PRLHR*	2834	NM_004248	CAUCGACCCUUACGCCUUU
si2				GGUCACAACUCCCGCCAAC
si3				CAGGGUUUCUGACUUAUUU
si4				GCAAACUGUUGGUCGCUUG
si1	*ASIC1*	41	NM_001095	GGAAAGUGCUACACGUUCA
si2				CUUCGAAGCAGGCAUCAAA
si3				CAACAACAGGUAUGAGAUA
si4				UCAACAAAUCUGAGCAAUA
si1	*CACNA1C*	775	NM_000719	GGAGGAGCACAUUCGAUAA
si2				GGAUGUUAGUCUGUAUUUA
si3				GGGUAGCAUUGUUGAUAUA
si4				GAAGAUGACUGCUUAUGGG
si1	*CHRNA1*	1134	NM_000079	GCCCAGACCUUGUUCUCUA
si2				UAACUGGCCUGGUAUUCUA
si3				GACCAGGAGUCUAACAAUG
si4				UAAAUCAGAUCGUGACAAC
si1	*GABRA3*	2556	NM_000808	GAGAUAAUCCGGUCUAGUA
si2				ACAAUGAGGUUAACAAUUC
si3				CGACUGAGACCAAGACCUA
si4				ACAAGUCACUGUUACAUGA
si1	*GRID2*	2895	NM_001510	GAGCGAUCCUUGUUAUGAA
si2				GGUAGGAGAACUUGUCUUU
si3				GGACUCACCCGGAGCAACA
si4				UCCUAGACUCUGCGGUAUA
si1	*GRIN3A*	116443	NM_133445	CGACGGAAAUACAUCUUUA
si2				CAGCUUACCGUAUGGAAUA
si3				CAACAUAUCCGAGCUAAUC
si4				GAAGAGUCCAUUUGGUUUG
si1	*KCNA7*	3743	NM_031886	GCGAAGAGGCUGGGAUGUU
si2				GAGACGCUGUGUAUUUGUU
si3				GGAAACACCUGGUCACCGA
si4				CACUGUGGGUGGCAAGAUA
si1	*KCNE2*	9992	NM_172201	GAACUUCUACUAUGUCAUC
si2				GACGGGAACACUCCAAUGA
si3				CGAAGGCCACCAUCCAUGA
si4				ACACAACAGCUGAGCAAGA
si1	*KCNIP2*	30819	NM_173197	GAAUGUCCCAGCGGAAUUG
si2				CAGCGUGGACGAUGAAUUU
si3				AAACCAAAUUCACGCGCAA
si4				GGAAUUCAUUGAGUCUUGU
si1	*KCNMB2*	10242	NM_005832	CCAACGUGCUGUUCCAUUC
si2				UCCAACGGAUCAAUAGAUA
si3				UCACACUCCUGCGCUCAUA
si4				GUACCUCUCCCUACUAUGU
si1	*MCOLN2*	255231	NM_153259	GCUCUAAGGUUACGGAAGA
si2				GACCAUACCAUGACAAGUU
si3				UCAGAUACCUGGGUUAUUU
si4				UCAGUCGUCUGUAUUUAUA

(Continued on next page)

TABLE 4 (Continued)

siRNA no.	Gene designation	Gene ID	GenBank accession no.	Target sequence
si1	*SCNN1D*	6339	NM_001130413.4	GCAUCAGGGUCAUGGUUCA
si2				GCUACUACCUCCACCCUCU
si3				GAGAAUGGAAGCAGCCACA
si4				CUACACAACACCUCCUACA

[a]A genome-wide RNAi screen was performed with siRNA SMARTpools to determine GPCR and IC gene hits for A/WSN/33-infected A549 cells. Hits were validated by deconvolution of the SMARTpools by testing each siRNA individually at a 50 nM final concentration. The table includes four siRNAs from each pool as well as relative gene sequence and target information. Gene hits were considered validated when two or more siRNAs yielded reduced viral replication when transfected individually.

phenyl) ethyl chloromethyl ketone [TPCK]-trypsin; Worthington, Columbus, OH). Infected cultures were incubated for 48 h at 37°C under 5% CO_2 and included siNTC and a siTOX siRNA control. siNTC (5′-UAGCGACUAAACACAUCAA-3′) targets no known sequence; siMAP2K (5′-PAGAACCUCCAUCCAUGUGCUU-3′, 5′-PUCAAAUCUGCUCUCUCUGCUU-3′, 5′-PAGUUGCUUCAAAUCUGCUCUU-3′, 5′-PAGAUGAAUUAGC UUUCUGGUU-3′), targeting MAP2K, which is required for influenza virus replication, was used a positive control, i.e., for host targeted decrease of influenza virus replication (45, 46); and siTOX was used to confirm siRNA transfection under transfection conditions. Following incubation, supernatants were collected and stored at −80°C until they were tested by plaque assays. For the selected gene targets, the two siRNAs that gave the greatest reduction in virus titers were used for all remaining studies.

Validated hits. A549 cells were transfected with individual OTP-siRNAs (2 siRNAs/gene target) from the deconvolution screen or with a control siRNA (siNTC, siMAP2K, or siTOX) at a final concentration of 50 nM in triplicate. Following transfection, the cells were infected with either A/WSN/33 (MOI, 0.01), A/CA/04/2009 (MOI, 0.1), or B/Yamagata/16/1988 (MOI, 0.1). The MOIs mediated low or no cytopathic effect (CPE). Following incubation, supernatants were removed and stored at −80°C until they were tested by plaque assays and $TCID_{50}$ assays. Two independent experiments were performed.

Cytotoxicity assay. Any cytotoxic effects associated with siRNA silencing were determined using a ToxiLight BioAssay kit (Lonza, Rockland, ME). Results were normalized to those with the siTOX transfection control, which results in complete cell death 48 h posttransfection. SMARTpools were considered toxic if transfection resulted in luminescence equivalent to ≥20% of the luminescence of the siTOX control.

Plaque assay. Infectious virus titers were determined by plaque assays as described elsewhere (47, 48, 91). Briefly, supernatants were serially diluted 10-fold in MEM with 1 μg/ml TPCK-trypsin and were inoculated onto 90% confluent MDCK cell monolayers in 12-well tissue culture plates (Corning Costar, Cambridge, MA). The virus was adsorbed for 1 h at 37°C under 5% CO_2 before the addition of 3 ml of overlay. The overlay medium contained 1 part liquid medium containing 10× MEM supplemented with 200 mm L-glutamine (Gibco), HEPES solution (Gibco), 7.5% $NaCHO_3$ (Gibco), penicillin-streptomycin-amphotericin B solution (Gibco), and 1 part 2.4% Avicel (FMC BioPolymer, Philadelphia, PA) in water or 1 part 1% agarose in water. Samples from A/WSN/33 or A/CA/04/2009 wells were incubated at 37°C under 5% CO_2 for 3 days. B/Yamagata/16/1988 was incubated at 37°C under 5% CO_2 for 5 days to allow for better plaque formation. The overlays were removed, the plates were washed twice with PBS, and the cell monolayers were fixed with acetone-methanol (80:20) for 20 min at RT. Following fixation, the plates were stained with crystal violet as described previously, and viral titers were determined (92, 93).

$TCID_{50}$ assay. Endpoint titers were determined by a $TCID_{50}$ assay as described previously (22, 25, 92). Briefly, supernatants collected from influenza virus-infected A549 cells were serially diluted 10-fold in triplicate on MDCK cells in 96-well plates. Influenza virus-infected MDCK cells were incubated 5 days using cell culture conditions described elsewhere (22, 25). Following incubation, an HA test was performed using 50 μl of supernatant from infected MDCK cells and 50 μl of 1% turkey red blood cells (RBC) for a final concentration of 0.5% in a round-bottom plate (97). The $TCID_{50}$ titers were calculated using the Reed and Muench method (92).

Hemagglutination assay. Hemagglutination was used for viral diagnosis of influenza viruses (92, 97). Briefly, 2-fold serial dilutions of virus in PBS were dispensed into individual wells of a 96-well round-bottom microtiter plate (Corning Costar, Cambridge, MA). Then aliquots of turkey RBC were added to each well to 0.5% of final volume. The highest dilution at which clumping was observed was regarded as the HA titer of the sample.

Statistics. HA assay results were normalized to results for siNTC-transfected controls. The nontargeting control was set to an arbitrary value of 1. Genes were specified a Z-score, calculated as $Z = (x - \mu)/(s/\sqrt{n})$, where x is equal to the average HA value of each gene, μ is equal to the population mean of the HA, s is equal to the standard deviation of each gene across the two independent experiments, and n is equal to the number of genes within the populations (16). Genes in the primary screen that were <1.5 standard deviations from the plate mean in both duplicates were considered primary hits.

ACKNOWLEDGMENTS

We would like to acknowledge funding in part from NIAID CEIRS contract numbers HHSN266200700006C and HHSN272201400004C to R.T. and from the Georgia Research Alliance to R.T.

REFERENCES

1. Jagger BW, Wise HM, Kash JC, Walters KA, Wills NM, Xiao YL, Dunfee RL, Schwartzman LM, Ozinsky A, Bell GL, Dalton RM, Lo A, Efstathiou S, Atkins JF, Firth AE, Taubenberger JK, Digard P. 2012. An overlapping protein-coding region in influenza A virus segment 3 modulates the host response. Science 337:199–204. https://doi.org/10.1126/science.1222213.
2. Shi M, Jagger BW, Wise HM, Digard P, Holmes EC, Taubenberger JK. 2012. Evolutionary conservation of the PA-X open reading frame in segment 3 of influenza A virus. J Virol 86:12411–12413. https://doi.org/10.1128/JVI.01677-12.
3. Wise HM, Barbezange C, Jagger BW, Dalton RM, Gog JR, Curran MD, Taubenberger JK, Anderson EC, Digard P. 2011. Overlapping signals for translational regulation and packaging of influenza A virus segment 2. Nucleic Acids Res 39:7775–7790. https://doi.org/10.1093/nar/gkr487.
4. Wise HM, Foeglein A, Sun J, Dalton RM, Patel S, Howard W, Anderson EC, Barclay WS, Digard P. 2009. A complicated message: identification of a novel PB1-related protein translated from influenza A virus segment 2 mRNA. J Virol 83:8021–8031. https://doi.org/10.1128/JVI.00826-09.
5. Yamayoshi S, Watanabe M, Goto H, Kawaoka Y. 2016. Identification of a novel viral protein expressed from the PB2 segment of influenza A virus. J Virol 90:444–456. https://doi.org/10.1128/JVI.02175-15.
6. Yang CW, Chen MF. 2016. Uncovering the potential pan proteomes encoded by genomic strand RNAs of influenza A viruses. PLoS One 11:e0146936. https://doi.org/10.1371/journal.pone.0146936.
7. Sandbulte MR, Westgeest KB, Gao J, Xu X, Klimov AI, Russell CA, Burke DF, Smith DJ, Fouchier RA, Eichelberger MC. 2011. Discordant antigenic drift of neuraminidase and hemagglutinin in H1N1 and H3N2 influenza viruses. Proc Natl Acad Sci U S A 108:20748–20753. https://doi.org/10.1073/pnas.1113801108.
8. Carrat F, Flahault A. 2007. Influenza vaccine: the challenge of antigenic drift. Vaccine 25:6852–6862. https://doi.org/10.1016/j.vaccine.2007.07.027.
9. World Health Organization. 2019. Influenza vaccines. https://www.who.int/biologicals/vaccines/influenza/en/. Accessed 29 July 2020.
10. World Health Organization. 2018. Influenza (seasonal). https://www.who.int/news-room/fact-sheets/detail/influenza-(seasonal). Accessed 29 July 2020.
11. Shrestha SS, Swerdlow DL, Borse RH, Prabhu VS, Finelli L, Atkins CY, Owusu-Edusei K, Bell B, Mead PS, Biggerstaff M, Brammer L, Davidson H, Jernigan D, Jhung MA, Kamimoto LA, Merlin TL, Nowell M, Redd SC, Reed C, Schuchat A, Meltzer MI. 2011. Estimating the burden of 2009 pandemic influenza A (H1N1) in the United States (April 2009–April 2010). Clin Infect Dis 52(Suppl 1):S75–S82. https://doi.org/10.1093/cid/ciq012.
12. Tricco A, Chit A, Soobiah C, Hallett D, Meier G, Chen M, Tashkandi M, Bauch C, Loeb M. 2013. Comparing influenza vaccine efficacy against mismatched and matched strains: a systematic review and meta-analysis. BMC Med 11:153. https://doi.org/10.1186/1741-7015-11-153.
13. Zimmerman RK, Nowalk MP, Chung J, Jackson ML, Jackson LA, Petrie JG, Monto AS, McLean HQ, Belongia EA, Gaglani M, Murthy K, Fry AM, Flannery B, U.S. Flu VE Investigators. 2016. 2014–2015 influenza vaccine effectiveness in the United States by vaccine type. Clin Infect Dis 63:1564–1573. https://doi.org/10.1093/cid/ciw635.
14. Shapira SD, Gat-Viks I, Shum BO, Dricot A, de Grace MM, Wu L, Gupta PB, Hao T, Silver SJ, Root DE, Hill DE, Regev A, Hacohen N. 2009. A physical and regulatory map of host-influenza interactions reveals pathways in H1N1 infection. Cell 139:1255–1267. https://doi.org/10.1016/j.cell.2009.12.018.
15. Fujioka Y, Tsuda M, Hattori T, Sasaki J, Sasaki T, Miyazaki T, Ohba Y. 2011. The Ras-PI3K signaling pathway is involved in clathrin-independent endocytosis and the internalization of influenza viruses. PLoS One 6:e16324. https://doi.org/10.1371/journal.pone.0016324.
16. Ehrhardt C, Marjuki H, Wolff T, Nurnberg B, Planz O, Pleschka S, Ludwig S. 2006. Bivalent role of the phosphatidylinositol-3-kinase (PI3K) during influenza virus infection and host cell defence. Cell Microbiol 8:1336–1348. https://doi.org/10.1111/j.1462-5822.2006.00713.x.
17. Planz O. 2013. Development of cellular signaling pathway inhibitors as new antivirals against influenza. Antiviral Res 98:457–468. https://doi.org/10.1016/j.antiviral.2013.04.008.
18. Yang JR, Lin YC, Huang YP, Su CH, Lo J, Ho YL, Yao CY, Hsu LC, Wu HS, Liu MT. 2011. Reassortment and mutations associated with emergence and spread of oseltamivir-resistant seasonal influenza A/H1N1 viruses in 2005–2009. PLoS One 6:e18177. https://doi.org/10.1371/journal.pone.0018177.
19. Sheu TG, Deyde VM, Okomo-Adhiambo M, Garten RJ, Xu X, Bright RA, Butler EN, Wallis TR, Klimov AI, Gubareva LV. 2008. Surveillance for neuraminidase inhibitor resistance among human influenza A and B viruses circulating worldwide from 2004 to 2008. Antimicrob Agents Chemother 52:3284–3292. https://doi.org/10.1128/AAC.00555-08.
20. Wathen MW, Barro M, Bright RA. 2013. Antivirals in seasonal and pandemic influenza—future perspectives. Influenza Other Respir Viruses 7(Suppl 1):76–80. https://doi.org/10.1111/irv.12049.
21. Hannon G. 2002. RNA interference. Nature 418:244–251. https://doi.org/10.1038/418244a.
22. Bakre A, Andersen LE, Meliopoulos V, Coleman K, Yan X, Brooks P, Crabtree J, Tompkins SM, Tripp RA. 2013. Identification of host kinase genes required for influenza virus replication and the regulatory role of microRNAs. PLoS One 8:e66796. https://doi.org/10.1371/journal.pone.0066796.
23. Meliopoulos VA, Andersen LE, Birrer KF, Simpson KJ, Lowenthal JW, Bean AG, Stambas J, Stewart CR, Tompkins SM, van Beusechem VW, Fraser I, Mhlanga M, Barichievy S, Smith Q, Leake D, Karpilow J, Buck A, Jona G, Tripp RA. 2012. Host gene targets for novel influenza therapies elucidated by high-throughput RNA interference screens. FASEB J 26:1372–1386. https://doi.org/10.1096/fj.11-193466.
24. Meliopoulos VA, Andersen LE, Brooks P, Yan X, Bakre A, Coleman JK, Tompkins SM, Tripp RA. 2012. MicroRNA regulation of human protease genes essential for influenza virus replication. PLoS One 7:e37169. https://doi.org/10.1371/journal.pone.0037169.
25. Perwitasari O, Johnson S, Yan X, Howerth E, Shacham S, Landesman Y, Baloglu E, McCauley D, Tamir S, Tompkins SM, Tripp RA. 2014. Verdinexor, a novel selective inhibitor of nuclear export, reduces influenza A virus replication in vitro and in vivo. J Virol 88:10228–10243. https://doi.org/10.1128/JVI.01774-14.
26. Zhang W, Tripp RA. 2008. RNA interference inhibits respiratory syncytial virus replication and disease pathogenesis without inhibiting priming of the memory immune response. J Virol 82:12221–12231. https://doi.org/10.1128/JVI.01557-08.
27. Karlas A, Machuy N, Shin Y, Pleissner KP, Artarini A, Heuer D, Becker D, Khalil H, Ogilvie LA, Hess S, Maurer AP, Muller E, Wolff T, Rudel T, Meyer TF. 2010. Genome-wide RNAi screen identifies human host factors crucial for influenza virus replication. Nature 463:818–822. https://doi.org/10.1038/nature08760.
28. Perwitasari O, Bakre A, Tompkins SM, Tripp RA. 2013. siRNA genome screening approaches to therapeutic drug repositioning. Pharmaceuticals (Basel) 6:124–160. https://doi.org/10.3390/ph6020124.
29. Zhou Y, Zhang C, Liang W. 2014. Development of RNAi technology for targeted therapy — a track of siRNA based agents to RNAi therapeutics. J Control Release 193:270–281. https://doi.org/10.1016/j.jconrel.2014.04.044.
30. Wu W, Orr-Burks N, Karpilow J, Tripp RA. 2017. Development of improved vaccine cell lines against rotavirus. Sci Data 4:170021. https://doi.org/10.1038/sdata.2017.21.
31. Murray J, Todd KV, Bakre A, Orr-Burks N, Jones L, Wu W, Tripp RA. 2017. A universal mammalian vaccine cell line substrate. PLoS One 12:e0188333. https://doi.org/10.1371/journal.pone.0188333.
32. van der Sanden SM, Wu W, Dybdahl-Sissoko N, Weldon WC, Brooks P, O'Donnell J, Jones LP, Brown C, Tompkins SM, Oberste MS, Karpilow J,

Tripp RA. 2016. Engineering enhanced vaccine cell lines to eradicate vaccine-preventable diseases: the polio end game. J Virol 90:1694–1704. https://doi.org/10.1128/JVI.01464-15.
33. Massirer KB, Perez SG, Mondol V, Pasquinelli AE. 2012. The miR-35-41 family of microRNAs regulates RNAi sensitivity in Caenorhabditis elegans. PLoS Genet 8:e1002536. https://doi.org/10.1371/journal.pgen.1002536.
34. Dupré DJ, Hébert TE, Jockers R (ed). 2012. GPCR signalling complexes: synthesis, assembly, trafficking and specificity. Springer, New York, NY.
35. Jakobsen M, Ellett A, Churchill M, Gorry P. 2010. Viral tropism, fitness and pathogenicity of HIV-1 subtype C. Future Virol 5:219–231. https://doi.org/10.2217/fvl.09.77.
36. Cilliers T, Willey S, Sullivan WM, Patience T, Pugach P, Coetzer M, Papathanasopoulos M, Moore JP, Trkola A, Clapham P, Morris L. 2005. Use of alternate coreceptors on primary cells by two HIV-1 isolates. Virology 339:136–144. https://doi.org/10.1016/j.virol.2005.05.027.
37. Morner A, Bjorndal A, Albert J, Kewalramani V, Littman D, Inoue R, Thorstensson R, Fenyo E, Bjorling E. 1999. Primary human immunodeficiency virus type 2 (HIV-2) isolates, like HIV-1 isolates, frequently use CCR5 but show promiscuity in coreceptor usage. J Virol 73:2343–2349. https://doi.org/10.1128/JVI.73.3.2343-2349.1999.
38. Cheng H, Lear-Rooney CM, Johansen L, Varhegyi E, Chen ZW, Olinger GG, Rong L. 2015. Inhibition of Ebola and Marburg virus entry by G protein-coupled receptor antagonists. J Virol 89:9932–9938. https://doi.org/10.1128/JVI.01337-15.
39. Bagal SK, Brown AD, Cox PJ, Omoto K, Owen RM, Pryde DC, Sidders B, Skerratt SE, Stevens EB, Storer RI, Swain NA. 2013. Ion channels as therapeutic targets: a drug discovery perspective. J Med Chem 56:593–624. https://doi.org/10.1021/jm3011433.
40. Hover S, King B, Hall B, Loundras EA, Taqi H, Daly J, Dallas M, Peers C, Schnettler E, McKimmie C, Kohl A, Barr JN, Mankouri J. 2016. Modulation of potassium channels inhibits bunyavirus infection. J Biol Chem 291:3411–3422. https://doi.org/10.1074/jbc.M115.692673.
41. Zheng K, Chen M, Xiang Y, Ma K, Jin F, Wang X, Wang X, Wang S, Wang Y. 2014. Inhibition of herpes simplex virus type 1 entry by chloride channel inhibitors tamoxifen and NPPB. Biochem Biophys Res Commun 446:990–996. https://doi.org/10.1016/j.bbrc.2014.03.050.
42. Hoffmann HH, Palese P, Shaw ML. 2008. Modulation of influenza virus replication by alteration of sodium ion transport and protein kinase C activity. Antiviral Res 80:124–134. https://doi.org/10.1016/j.antiviral.2008.05.008.
43. O'Grady SM, Lee SY. 2003. Chloride and potassium channel function in alveolar epithelial cells. Am J Physiol Lung Cell Mol Physiol 284:L689–L700. https://doi.org/10.1152/ajplung.00256.2002.
44. Schuitemaker H, Koot M, Kootstra NA, Dercksen MW, de Goede RE, van Steenwijk RP, Lange JM, Schattenkerk JK, Miedema F, Tersmette M. 1992. Biological phenotype of human immunodeficiency virus type 1 clones at different stages of infection: progression of disease is associated with a shift from monocytotropic to T-cell-tropic virus populations. J Virol 66:1354–1360. https://doi.org/10.1128/JVI.66.3.1354-1360.1992.
45. Liu R, Paxton W, Choe S, Ceradini D, Martin S, Horuk R, MacDonald M, Stuhlmann H, Koup R, Landau N. 1996. Homozygous defect in HIV-1 coreceptor accounts for resistance of some multiply-exposed individuals to HIV-1 infection. Cell Press 86:367–377. https://doi.org/10.1016/S0092-8674(00)80110-5.
46. Samson M, Libert F, Doranz BJ, Rucker J, Liesnard C, Farber CM, Saragosti S, Lapoumeroulie C, Cognaux J, Forceille C, Muyldermans G, Verhofstede C, Burtonboy G, Georges M, Imai T, Rana S, Yi Y, Smyth RJ, Collman RG, Doms RW, Vassart G, Parmentier M. 1996. Resistance to HIV-1 infection in Caucasian individuals bearing mutant alleles of the CCR-5 chemokine receptor gene. Nature 382:722–725. https://doi.org/10.1038/382722a0.
47. Paulsen RD, Soni DV, Wollman R, Hahn AT, Yee MC, Guan A, Hesley JA, Miller SC, Cromwell EF, Solow-Cordero DE, Meyer T, Cimprich KA. 2009. A genome-wide siRNA screen reveals diverse cellular processes and pathways that mediate genome stability. Mol Cell 35:228–239. https://doi.org/10.1016/j.molcel.2009.06.021.
48. Jackson AL, Burchard J, Leake D, Reynolds A, Schelter J, Guo J, Johnson JM, Lim L, Karpilow J, Nichols K, Marshall W, Khvorova A, Linsley PS. 2006. Position-specific chemical modification of siRNAs reduces "off-target" transcript silencing. RNA 12:1197–1205. https://doi.org/10.1261/rna.30706.
49. Pleschka S, Wolff T, Ehrhardt C, Hobom G, Planz O, Rapp UR, Ludwig S. 2001. Influenza virus propagation is impaired by inhibition of the Raf/MEK/ERK signalling cascade. Nat Cell Biol 3:301–305. https://doi.org/10.1038/35060098.
50. Ludwig S, Wolff T, Ehrhardt C, Wurzer WJ, Reinhardt J, Planz O, Pleschka S. 2004. MEK inhibition impairs influenza B virus propagation without emergence of resistant variants. FEBS Lett 561:37–43. https://doi.org/10.1016/S0014-5793(04)00108-5.
51. Camerino DC, Tricarico D, Desaphy J-F. 2007. Ion channel pharmacology. Neurotherapeutics 4:184–198. https://doi.org/10.1016/j.nurt.2007.01.013.
52. Yan AWC, Zhou J, Beauchemin CAA, Russell CA, Barclay WS, Riley S. 2020. Quantifying mechanistic traits of influenza viral dynamics using in vitro data. Epidemics 33:100406. https://doi.org/10.1016/j.epidem.2020.100406.
53. Henle W, Rosenberg E. 1949. One-step growth curves of various strains of influenza A and B viruses and their inhibition by inactivated virus of the homologous type. J Exp Med 89:279–285. https://doi.org/10.1084/jem.89.3.279.
54. Stertz S, Shaw ML. 2011. Uncovering the global host cell requirements for influenza virus replication via RNAi screening. Microbes Infect 13:516–525. https://doi.org/10.1016/j.micinf.2011.01.012.
55. Sodhi A, Montaner S, Gutkind JS. 2004. Viral hijacking of G-protein-coupled-receptor signalling networks. Nat Rev Mol Cell Biol 5:998–1012. https://doi.org/10.1038/nrm1529.
56. Skehel J, Wiley D. 2000. Receptor binding and membrane fusion in virus entry: the influenza hemagglutinin. Annu Rev Biochem 69:531–569. https://doi.org/10.1146/annurev.biochem.69.1.531.
57. Yoshimura A, Ohnishi S. 1984. Uncoating of influenza virus in endosomes. J Virol 51:497–504. https://doi.org/10.1128/JVI.51.2.497-504.1984.
58. Imming P, Sinning C, Meyer A. 2006. Drugs, their targets and the nature and number of drug targets. Nat Rev Drug Discov 5:821–834. https://doi.org/10.1038/nrd2132.
59. Reference deleted.
60. PubChem. 2016. Gene Summary: SCNN1D — sodium channel epithelial 1 delta subunit (human), on NCBI. https://pubchem.ncbi.nlm.nih.gov/gene/SCNN1D/human.
61. Heynisch B, Frensing T, Heinze K, Seitz C, Genzel Y, Reichl U. 2010. Differential activation of host cell signalling pathways through infection with two variants of influenza A/Puerto Rico/8/34 (H1N1) in MDCK cells. Vaccine 28:8210–8218. https://doi.org/10.1016/j.vaccine.2010.07.076.
62. Pan C, Kumar C, Bohl S, Klingmueller U, Mann M. 2009. Comparative proteomic phenotyping of cell lines and primary cells to assess preservation of cell type-specific functions. Mol Cell Proteomics 8:443–450. https://doi.org/10.1074/mcp.M800258-MCP200.
63. Luttrell LM. 2008. Reviews in molecular biology and biotechnology: transmembrane signaling by G protein-coupled receptors. Mol Biotechnol 39:239–264. https://doi.org/10.1007/s12033-008-9031-1.
64. George SR, O'Dowd BF, Lee SP. 2002. G-protein-coupled receptor oligomerization and its potential for drug discovery. Nat Rev Drug Discov 1:808–820. https://doi.org/10.1038/nrd913.
65. Downes GB, Gautam N. 1999. The G protein subunit gene families. Genomics 62:544–552. https://doi.org/10.1006/geno.1999.5992.
66. Dumaz N, Marais R. 2005. Integrating signals between cAMP and the RAS/RAF/MEK/ERK signalling pathways. Based on the anniversary prize of the Gesellschaft für Biochemie und Molekularbiologie Lecture delivered on 5 July 2003 at the Special FEBS Meeting in Brussels. FEBS J 272:3491–3504. https://doi.org/10.1111/j.1742-4658.2005.04763.x.
67. Hui E, Nayak DP. 2002. Role of G protein and protein kinase signalling in influenza virus budding in MDCK cells. J Gen Virol 83:3055–3066. https://doi.org/10.1099/0022-1317-83-12-3055.
68. De Matteis M, Santini G, Kahn R, Tullio G, Luini A. 1993. Receptor and protein kinase C-mediated regulation of ARF binding to the Golgi complex. Nature 364:818–820. https://doi.org/10.1038/364818a0.
69. Pimplikar S, Simons K. 1994. Activators of protein kinase A stimulate apical but not basolateral transport in epithelial Madin-Darby canine kidney cells. J Biol Chem 269:19054–19059. https://doi.org/10.1016/S0021-9258(17)32273-1.
70. Little PJ, Neylon CB, Tkachuk VA, Bobik A. 1992. Endothelin-1 and endothelin-3 stimulate calcium mobilization by different mechanisms in vascular smooth muscle. Biochem Biophys Res Commun 183:694–700. https://doi.org/10.1016/0006-291X(92)90538-V.
71. Fujioka Y, Tsuda M, Nanbo A, Hattori T, Sasaki J, Sasaki T, Miyazaki T, Ohba Y. 2013. A Ca^{2+}-dependent signalling circuit regulates influenza A virus internalization and infection. Nat Commun 4:2763. https://doi.org/10.1038/ncomms3763.

72. Lum A, Wang B, Beck-Engeser G, Li L, Channa N, Wabl M. 2010. Orphan receptor GPR110, an oncogene overexpressed in lung and prostate cancer. BMC Cancer 10:40. https://doi.org/10.1186/1471-2407-10-40.
73. Fredriksson R, Lagerstro M, Hoglund P, Schioth H. 2002. Novel human G protein-coupled receptors with long N-terminals containing GPS domains and Ser/Thr-rich regions. FEBS Lett 531:407–414. https://doi.org/10.1016/S0014-5793(02)03574-3.
74. Carmon KS, Gong X, Lin Q, Thomas A, Liu Q. 2011. R-spondins function as ligands of the orphan receptors LGR4 and LGR5 to regulate Wnt/beta-catenin signaling. Proc Natl Acad Sci U S A 108:11452–11457. https://doi.org/10.1073/pnas.1106083108.
75. Okinaga S, Slattery D, Humbles A, Zsengeller Z, Morteau O, Kinrade M, Brodbeck R, Krause J, Choe H-R, Gerard N, Gerard C. 2003. C5L2, a nonsignaling C5A binding protein. Biochemistry 42:9406–9415. https://doi.org/10.1021/bi034489v.
76. Van Lith LH, Oosterom J, Van Elsas A, Zaman GJ. 2009. C5a-stimulated recruitment of beta-arrestin2 to the nonsignaling 7-transmembrane decoy receptor C5L2. J Biomol Screen 14:1067–1075. https://doi.org/10.1177/1087057109341407.
77. Berdiev BK, Xia J, Jovov B, Markert JM, Mapstone TB, Gillespie GY, Fuller CM, Bubien JK, Benos DJ. 2002. Protein kinase C isoform antagonism controls BNaC2 (ASIC1) function. J Biol Chem 277:45734–45740. https://doi.org/10.1074/jbc.M208995200.
78. Yuzaki M. 2004. The δ2 glutamate receptor: a key molecule controlling synaptic plasticity and structure in Purkinje cells. Cerebellum 3:89–93. https://doi.org/10.1080/14734220410028921.
79. Butterworth MB. 2010. Regulation of the epithelial sodium channel (ENaC) by membrane trafficking. Biochim Biophys Acta 1802:1166–1177. https://doi.org/10.1016/j.bbadis.2010.03.010.
80. Ji HL, Song W, Gao Z, Su XF, Nie HG, Jiang Y, Peng JB, He YX, Liao Y, Zhou YJ, Tousson A, Matalon S. 2009. SARS-CoV proteins decrease levels and activity of human ENaC via activation of distinct PKC isoforms. Am J Physiol Lung Cell Mol Physiol 296:L372–L383. https://doi.org/10.1152/ajplung.90437.2008.
81. Liu Y, Guo F, Dai M, Wang D, Tong Y, Huang J, Hu J, Li G. 2009. Gammaaminobutyric acid A receptor alpha 3 subunit is overexpressed in lung cancer. Pathol Oncol Res 15:351–358. https://doi.org/10.1007/s12253-008-9128-7.
82. Law AH, Lee DC, Yuen KY, Peiris M, Lau AS. 2010. Cellular response to influenza virus infection: a potential role for autophagy in CXCL10 and interferon-alpha induction. Cell Mol Immunol 7:263–270. https://doi.org/10.1038/cmi.2010.25.
83. Rinkenberger N, Schoggins JW. 2018. Mucolipin-2 cation channel increases trafficking efficiency of endocytosed viruses. mBio 9:e02314-17. https://doi.org/10.1128/mBio.02314-17.
84. Dorsam RT, Murugappan S, Ding Z, Kunapuli SP. 2003. Clopidogrel: interactions with the P2Y12 receptor and clinical relevance. Hematology 8:359–365. https://doi.org/10.1080/10245330310001621260.
85. Savi P, Zachayus JL, Delesque-Touchard N, Labouret C, Herve C, Uzabiaga MF, Pereillo JM, Culouscou JM, Bono F, Ferrara P, Herbert JM. 2006. The active metabolite of clopidogrel disrupts P2Y12 receptor oligomers and partitions them out of lipid rafts. Proc Natl Acad Sci U S A 103:11069–11074. https://doi.org/10.1073/pnas.0510446103.
86. Storey RF. 2001. The P2Y12 receptor as a therapeutic target in cardiovascular disease. Platelets 12:197–209. https://doi.org/10.1080/09537100120058739.
87. Elkahloun AG, Saavedra JM. 2020. Candesartan could ameliorate the COVID-19 cytokine storm. Biomed Pharmacother 131:110653. https://doi.org/10.1016/j.biopha.2020.110653.
88. Zhang H, Baker A. 2017. Recombinant human ACE2: acing out angiotensin II in ARDS therapy. Crit Care 21:305. https://doi.org/10.1186/s13054-017-1882-z.
89. Gong MJ, Chang YY, Shao JJ, Li SF, Zhang YG, Chang HY. 2019. Antiviral effect of amiloride on replication of foot and mouth disease virus in cell culture. Microb Pathog 135:103638. https://doi.org/10.1016/j.micpath.2019.103638.
90. Jones NG, Slater R, Cadiou H, McNaughton P, McMahon SB. 2004. Acid-induced pain and its modulation in humans. J Neurosci 24:10974–10979. https://doi.org/10.1523/JNEUROSCI.2619-04.2004.
91. Woolcock PR. 2008. Avian influenza virus isolation and propagation in chicken eggs. Methods Mol Biol 436:35–46. https://doi.org/10.1007/978-1-59745-279-3_6.
92. Reed LJ, Muench H. 1938. A simple method of estimating fifty percent endpoints. Am J Hyg 27:493–497. https://doi.org/10.1093/oxfordjournals.aje.a118408.
93. Klimov A, Balish A, Veguilla V, Sun H, Schiffer J, Lu X, Katz JM, Hancock K. 2012. Influenza virus titration, antigenic characterization, and serological methods for antibody detection. Methods Mol Biol 865:25–51. https://doi.org/10.1007/978-1-61779-621-0_3.
94. Appleyard G, Maber HB. 1974. Plaque formation by influenza viruses in the presence of trypsin. J Gen Virol 25:351–357. https://doi.org/10.1099/0022-1317-25-3-351.
95. Pei Y, Tuschl T. 2006. On the art of identifying effective and specific siRNAs. Nat Methods 3:670–676. https://doi.org/10.1038/nmeth911.
96. Haney S. 2007. Increasing the robustness and validity of RNAi screens. Pharmacogenomics 8:1037–1049. https://doi.org/10.2217/14622416.8.8.1037.
97. Hirst GK. 1942. The quantitative determination of influenza virus and antibodies by means of red cell agglutination. J Exp Med 75:49–64. https://doi.org/10.1084/jem.75.1.49.
98. Schwabe U, Ukena D, Lohse MJ. 1985. Xanthine derivatives as antagonists at A_1 and A_2 adenosine receptors. Naunyn Schmiedebergs Arch Pharmacol 330:212–221. https://doi.org/10.1007/BF00572436.
99. Daly J, Jacobson KA, Ukena D. 1987. Adenosine receptors: development of selective agonists and antagonists. Prog Clin Biol Res 230:41–63.
100. Kreth S, Ledderose C, Luchting B, Weis F, Thiel M. 2010. Immunomodulatory properties of pentoxifylline are mediated via adenosine-dependent pathways. Shock 34:10–16. https://doi.org/10.1097/SHK.0b013e3181cdc3e2.
101. Miura S, Matsuo Y, Nakayama A, Tomita S, Suematsu Y, Saku K. 2014. Ability of the new AT1 receptor blocker azilsartan to block angiotensin II-induced AT1 receptor activation after wash-out. J Renin Angiotensin Aldosterone Syst 15:7–12. https://doi.org/10.1177/1470320313482170.
102. Chen X, Ji ZL, Chen YZ. 2002. TTD: Therapeutic Target Database. Nucleic Acids Res 30:412–415. https://doi.org/10.1093/nar/30.1.412.
103. Vauquelin G, Fierens F, Van Liefde I. 2006. Long-lasting angiotensin type 1 receptor binding and protection by candesartan: comparison with other biphenyl-tetrazole sartans. J Hypertens Suppl 24:S23–S30. https://doi.org/10.1097/01.hjh.0000220403.61493.18.
104. Hope S, Brecher P, Chobanian AV. 1999. Comparison of the effects of AT1 receptor blockade and angiotensin converting enzyme inhibition on atherosclerosis. Am J Hypertens 12:28–34. https://doi.org/10.1016/S0895-7061(98)00203-9.
105. Adams MA, Trudeau L. 2000. Irbesartan: review of pharmacology and comparative properties. Can J Clin Pharmacol 7:22–31.
106. Criscione L, de Gasparo M, Bühlmayer P, Whitebread S, Ramjoué HP, Wood J. 1993. Pharmacological profile of valsartan: a potent, orally active, nonpeptide antagonist of the angiotensin II AT, receptor subtype. Br J Pharmacol 110:761–771. https://doi.org/10.1111/j.1476-5381.1993.tb13877.x.
107. Shahid M, Walker GB, Zorn SH, Wong EHF. 2009. Asenapine: a novel psychopharmacologic agent with a unique human receptor signature. J Psychopharmacol 23:65–73. https://doi.org/10.1177/0269881107082944.
108. Gan XD, Wei BZ, Fang D, Fang Q, Li KY, Ding SL, Peng S, Wan J. 2015. Efficacy and safety analysis of new P2Y12 inhibitors versus clopidogrel in patients with percutaneous coronary intervention: a meta-analysis. Curr Med Res Opin 31:2313–2323. https://doi.org/10.1185/03007995.2015.1098600.
109. Boeynaems JM, van Giezen H, Savi P, Herbert JM. 2005. P2Y receptor antagonists in thrombosis. Curr Opin Investig Drugs 6:275–282.
110. Zhan C, Yang J, Dong XC, Wang YL. 2007. Molecular modeling of purinergic receptor P2Y12 and interaction with its antagonists. J Mol Graph Model 26:20–31. https://doi.org/10.1016/j.jmgm.2006.09.006.
111. Taubert D, Kastrati A, Harlfinger S, Gorchakova O, Lazar A, von Beckerath N, Schomig A, Schomig E. 2004. Pharmacokinetics of clopidogrel after administration of a high loading dose. Thromb Haemost 92:311–316. https://doi.org/10.1160/TH04-02-0105.
112. Dovlatova NL, Jakubowski JA, Sugidachi A, Heptinstall S. 2008. The reversible P2Y antagonist cangrelor influences the ability of the active metabolites of clopidogrel and prasugrel to produce irreversible inhibition of platelet function. J Thromb Haemost 6:1153–1159. https://doi.org/10.1111/j.1538-7836.2008.03020.x.
113. Teng R. 2015. Ticagrelor: pharmacokinetic, pharmacodynamic and pharmacogenetic profile: an update. Clin Pharmacokinet 54:1125–1138. https://doi.org/10.1007/s40262-015-0290-2.

114. Bruck H, Poller U, Lussenhop H, Ponicke K, Temme T, Heusch G, Philipp T, Brodde OE. 2004. Beta 2-adrenoceptor-mediated intrinsic sympathomimetic activity of carteolol: an in vivo study. Naunyn Schmiedebergs Arch Pharmacol 370:361–368. https://doi.org/10.1007/s00210-004-0988-4.
115. Quast U, Vollmer KO. 1984. Binding of beta-adrenoceptor antagonists to rat and rabbit lung: special reference to levobunolol. Arzneimittelforschung 34:579–584.
116. Overington JP, Al-Lazikani B, Hopkins AL. 2006. How many drug targets are there? Nat Rev Drug Discov 5:993–996. https://doi.org/10.1038/nrd2199.
117. Joseph SS, Lynham JA, Colledge WH, Kaumann AJ. 2004. Binding of (–)-[3H]-CGP12177 at two sites in recombinant human beta 1-adrenoceptors and interaction with beta-blockers. Naunyn Schmiedebergs Arch Pharmacol 369:525–532. .
118. Rotmensch HH, Vlasses PH, Feinberg JA, Abrams WB, Ferguson RK. 1993. Comparisons of beta-adrenergic blocking properties of S- and R-timolol in humans. J Clin Pharmacol 33:544–548. https://doi.org/10.1002/j.1552-4604.1993.tb04701.x.
119. Shimatani T, Inoue M, Kuroiwa T, Xu J, Nakamura M, Tazuma S, Ikawa K, Morikawa N. 2006. Lafutidine, a newly developed antiulcer drug, elevates postprandial intragastric pH and increases plasma calcitonin gene-related peptide and somatostatin concentrations in humans: comparisons with famotidine. Dig Dis Sci 51:114–120. https://doi.org/10.1007/s10620-006-3094-2.
120. Chremos AN. 1987. Clinical pharmacology of famotidine: a summary. J Clin Gastroenterol 9:7–12. https://doi.org/10.1097/00004836-198707002-00003.
121. Voilley N, de Weille J, Mamet J, Lazdunski M. 2001. Nonsteroid anti-inflammatory drugs inhibit both the activity and the inflammation-induced expression of acid-sensing ion channels in nociceptors. J Neurosci 21:8026–8033. https://doi.org/10.1523/JNEUROSCI.21-20-08026.2001.
122. Du L, Roberts JD, Jr. 2019. Transforming growth factor-β downregulates sGC subunit expression in pulmonary artery smooth muscle cells via MEK and ERK signaling. Am J Physiol Lung Cell Mol Physiol 316:L20–L34. https://doi.org/10.1152/ajplung.00319.2018.
123. Reversi A, Rimoldi V, Marrocco T, Cassoni P, Bussolati G, Parenti M, Chini B. 2005. The oxytocin receptor antagonist atosiban inhibits cell growth via a "biased agonist" mechanism. J Biol Chem 280:16311–16318. https://doi.org/10.1074/jbc.M409945200.
124. Kim SH, MacIntyre DA, Hanyaloglu AC, Blanks AM, Thornton S, Bennett PR, Terzidou V. 2016. The oxytocin receptor antagonist, Atosiban, activates pro-inflammatory pathways in human amnion via $G_{\alpha i}$ signalling. Mol Cell Endocrinol 420:11–23. https://doi.org/10.1016/j.mce.2015.11.012.
125. Yamamura H, Ugawa S, Ueda T, Shimada S. 2005. Evans blue is a specific antagonist of the human epithelial Na^+ channel delta-subunit. J Pharmacol Exp Ther 315:965–969. https://doi.org/10.1124/jpet.105.092775.
126. Wagner CA, Ott M, Klingel K, Beck S, Melzig J, Friedrich B, Wild KN, Bröer S, Moschen I, Albers A, Waldegger S, Tümmler B, Egan ME, Geibel JP, Kandolf R, Lang F. 2001. Effects of the serine/threonine kinase SGK1 on the epithelial Na^+ channel (ENaC) and CFTR: implications for cystic fibrosis. Cell Physiol Biochem 11:209–218. https://doi.org/10.1159/000051935.
127. Elkahloun AG, Saavedra JM. 2020. Candesartan could ameliorate the COVID-19 cytokine storm. Biomed Pharmacother 131:110653. https://doi.org/10.1016/j.biopha.2020.110653.
128. Sriram K, Loomba R, Insel PA. 2020. Targeting the renin-angiotensin signaling pathway in COVID-19: unanswered questions, opportunities, and challenges. Proc Natl Acad Sci U S A 117:29274–29282. https://doi.org/10.1073/pnas.2009875117.
129. Sriram K, Insel PA. 2020. A hypothesis for pathobiology and treatment of COVID-19: the centrality of ACE1/ACE2 imbalance. Br J Pharmacol 177:4825–4844. https://doi.org/10.1111/bph.15082.